

Gradient flows without blow-up for Lefschetz thimbles

Yuya Tanizaki,^a Hiromichi Nishimura,^a and Jacobus J. M. Verbaarschot^b

^a*RIKEN BNL Research Center, Brookhaven National Laboratory, Upton, NY 11973 USA*

^b*Department of Physics and Astronomy, Stony Brook University, Stony Brook, NY 11794, USA*

E-mail: yuya.tanizaki@riken.jp, hnishimura@bnl.gov,
Jacobus.Verbaarschot@stonybrook.edu

ABSTRACT: We propose new gradient flows that define Lefschetz thimbles and do not blow up in a finite flow time. We study analytic properties of these gradient flows, and confirm them by numerical tests in simple examples.

Contents

1	Introduction	1
2	Blow-up of conventional gradient flows for Lefschetz thimbles	3
2.1	Brief review of Lefschetz-thimble methods for sign problems	3
2.2	Blow-up of conventional flows	5
3	Proposal of new gradient flows without blow-up	6
3.1	Justification of new gradient flows	7
3.2	Proof of the absence of blow-up	8
3.3	On the choice of Λ_B and Λ_F	9
4	Numerical tests in simple examples	10
4.1	Airy integral	10
4.2	Gaussian model with fermion determinant	12
4.2.1	Case 1	12
4.2.2	Case 2	14
4.3	$U(1)$ one-link model	16
4.3.1	Small κ	16
4.3.2	Large κ	18
5	Conclusions	19
A	Proof of equivalence among gradient flows	20
B	Flow equation for the Jacobian matrix	22
C	Comment on the Hermitian and Kähler metric in the gradient flow	23
C.1	Quick review on complex structure	23
C.1.1	Hermitian structure	23
C.1.2	Kähler structure	24
C.2	Gradient flow and Hamilton equation of motion	24

1 Introduction

To study properties of strongly-correlated many-body systems, numerical simulation provides us powerful tools. Exact diagonalization of the Hamiltonian gives the complete information of physical systems, however it requires an exponentially large amount of the computational cost as the number of particles increases. Monte Carlo simulation of the path

integral circumvents this problem, and many physical systems of hadron and condensed-matter physics in thermal equilibrium have been successfully studied with this method [1–4].

Monte Carlo simulation is based on importance sampling, and thus the Boltzmann weight $\exp(-S)$ with the classical action S must be positive semi-definite. The Boltzmann weight in many interesting systems, however, takes on complex values, so that the idea of importance sampling cannot be applied, which is called the sign problem [5, 6]. The conventional solution of this problem is the reweighting method with phase quenching, but this procedure generally revives the exponential complexity and its use is very limited [7]. In hadron physics, high-density cold nuclear matter gets a lot of attention because of its relevance to neutron-star physics [8], but finite-density quantum chromodynamics (QCD) suffers from the sign problem, and we do not have a technique for *ab initio* computations of this theory [9].

Recently, a new systematic approach to the sign problem has been developing based on the complexification of path-integral variables, and it is called the Lefschetz-thimble Monte Carlo method [10–36]. If the integration variables are complexified, there is a great deal of freedom in the choice of integration contours thanks to Cauchy’s theorem. Although expectation values of physical observables does not change under the continuous deformation of integration contours, the strength of the sign problem heavily depends on the choice of contours, so we can expect that there must be an optimal choice. For one-dimensional integrals, it is given by the stationary-phase path, and its higher dimensional analogue is called the Lefschetz thimble. This technique has been developed in the context of the hyperasymptotics of multi-dimensional exponential integrals [37–39], and it is now applied in physics not only to the sign problem but also to the resurgence theory [40–62]. Quite recently, the Lefschetz-thimble method is also discussed in the context of quantum cosmology [63, 64] through its application to the real-time quantum phenomena [17, 18, 31].

In order to find Lefschetz thimbles, all we have to do is to analyze the gradient flow in the space of complexified field configurations $z^i = x^i + iy^i$ [40, 41]:

$$\frac{dz^i}{dt} = \overline{\left(\frac{\partial S(z)}{\partial z^i}\right)}. \quad (1.1)$$

However, as we will see in this paper, solutions of the gradient flow (1.1) generically blow up within finite-time intervals, so one must treat them carefully in numerical computations to get the correct answer. Instead, we propose a new gradient flow equation,

$$\frac{dz^i}{dt} = e^{-2\text{Re}(S_B(z))/\Lambda_B} \frac{|D(z)|^2}{|D(z)|^2 + \Lambda_F^{-2}} \overline{\left(\frac{\partial S(z)}{\partial z^i}\right)}, \quad (1.2)$$

where S_B is the bosonic classical action, D is the fermionic determinant, and the total classical action is $S = S_B - \ln D$. Here, Λ_B and Λ_F are positive real parameters to be tuned appropriately. This new flow equation (1.2) turns out to define the Lefschetz-thimble decomposition of the original integration as the conventional one (1.1) does, and all of its solutions do not show blow-up.

This paper is organized as follows: Section 2 gives a brief review on the Lefschetz-thimble method with the conventional gradient flow, and we argue that blow-up generically

happens using simple examples. In Sec. 3, we introduce new gradient flows and justify their use for the Lefschetz-thimble method. Furthermore, we show that blow-up does not occur in that new flow equation. In Sec. 4, we numerically study the gradient flow in simple examples to see its behaviors and check that the sign problem is indeed equally solved compared with the conventional gradient flow. Concluding remarks are made in Sec. 5. Several technical details are worked out in two appendices. In appendix A, we give a mathematical proof on the equivalence among gradient flows. The deviation equation of the gradient flow to compute the Jacobian is given in Appendix B, and in Appendix C, we discuss some technical details on the complex structure to claim that our proposal works with gauge symmetries.

2 Blow-up of conventional gradient flows for Lefschetz thimbles

We first review the Lefschetz-thimble approach to the sign problem in Sec. 2.1. In Sec. 2.2, we explain that the gradient flow conventionally used blows up in a finite time by demonstrating it in simple two examples.

2.1 Brief review of Lefschetz-thimble methods for sign problems

Let us consider the following integral,

$$Z = \int_{\mathbb{R}^n} d^n x \exp[-S(x)], \quad (2.1)$$

where the action $S(x)$ is a complex-valued polynomial in x . Since $S(x)$ is complex valued, this integral becomes oscillatory and the sign problem appears. The Lefschetz-thimble method is a method to make the sign problem milder by deforming the integration contour \mathbb{R}^n to other n -dimensional submanifolds of the complexified space \mathbb{C}^n .

Conventionally, such submanifolds are constructed by solving the following gradient flow [10–36],

$$\frac{dz^i}{dt} = \overline{\left(\frac{\partial S(z)}{\partial z^i} \right)}, \quad (2.2)$$

where z^i is a holomorphic coordinate of \mathbb{C}^n : $z^i = x^i + iy^i$. We can understand why (2.2) is called the gradient flow as follows: Let us pick up the standard (Kähler) metric $ds^2 = \delta_{i\bar{j}} dz^i \otimes d\bar{z}^j$, then (2.2) is indeed the gradient flow with the height function $h(z, \bar{z}) = 2\text{Re}(S(z))$,

$$\frac{dz^i}{dt} = \delta^{i\bar{j}} \frac{\partial}{\partial z^j} h(z, \bar{z}). \quad (2.3)$$

Therefore, $\text{Re}(S(z)) = \frac{1}{2}h(z, \bar{z})$ monotonically increases along the flow (2.2). Another important property of (2.2) is that $\text{Im}(S(z))$ is constant along the flow,

$$\frac{d}{dt} \text{Im}(S(z)) = 0, \quad (2.4)$$

because of the holomorphy of $S(z)$.

Let $\{z_\sigma\}_{\sigma \in \Sigma}$ be the set of the saddle points, $\partial S(z_\sigma) = 0$. Using the gradient flow (2.2), we define the Lefschetz thimble and its dual by [10, 14, 17, 40, 41]

$$\mathcal{J}_\sigma = \{z(0) \in \mathbb{C}^n \mid z(-\infty) = z_\sigma\}, \mathcal{K}_\sigma = \{z(0) \in \mathbb{C}^n \mid z(+\infty) = z_\sigma\}, \quad (2.5)$$

respectively. The claim from the Picard–Lefschetz theory is that we can compute relative homologies as [37–41]

$$H_n(\mathbb{C}^n, \{e^{-\operatorname{Re}(S)} \ll 1\}) \simeq \sum_{\sigma} \mathbb{Z} \mathcal{J}_\sigma, \quad (2.6)$$

$$H_n(\mathbb{C}^n, \{e^{-\operatorname{Re}(S)} \gg 1\}) \simeq \sum_{\sigma} \mathbb{Z} \mathcal{K}_\sigma, \quad (2.7)$$

if $S(z)$ satisfy certain properties. By imposing appropriate orientations to \mathcal{J}_σ and \mathcal{K}_σ , the intersection pairing satisfies

$$\langle \mathcal{J}_\sigma, \mathcal{K}_\tau \rangle = \delta_{\sigma\tau}, \quad (2.8)$$

and thus we can compute the homology class of the original integration cycle \mathbb{R}^n as

$$[\mathbb{R}^n] = \sum_{\sigma \in \Sigma} \langle \mathbb{R}^n, \mathcal{K}_\sigma \rangle [\mathcal{J}_\sigma], \quad (2.9)$$

where $[\mathcal{J}]$ represents the homology class of the cycle \mathcal{J} . As a result, we can rewrite the original integration as

$$Z = \sum_{\sigma} \langle \mathbb{R}^n, \mathcal{K}_\sigma \rangle \int_{\mathcal{J}_\sigma} d^n z \exp[-S(z)]. \quad (2.10)$$

Since $\operatorname{Im}(S(z))$ is constant along each Lefschetz thimble \mathcal{J}_σ , the sign problem of (2.10) can be absent or much milder than that of the original integral (2.1).

There is a practical way to realize the decomposition (2.10), and we introduce it following Refs. [30, 31]. Let $z(t, x)$ be the solution of (2.2) with the initial condition $z(0, x) = x$. We fix the flow time T , and define the n -dimensional submanifold by

$$\mathcal{J}(T) = \{z(T, x) \in \mathbb{C}^n \mid x \in \mathbb{R}^n\}. \quad (2.11)$$

Thanks to Cauchy’s theorem, we obtain

$$Z = \int_{\mathcal{J}(T)} dz \exp[-S(z)] = \int_{\mathbb{R}^n} d^n x \det \left(\frac{\partial z^i(T, x)}{\partial x^j} \right) \exp[-S(z(T, x))]. \quad (2.12)$$

The first identity means that $\mathcal{J}(T)$ belongs to the same homology class as \mathbb{R}^n . Furthermore, if T is sufficiently large, $\mathcal{J}(T)$ would become almost identical to the sum of Lefschetz thimbles. Therefore, the last expression of (2.12) can be regarded as a realization of the Lefschetz-thimble decomposition (2.10) when T is large enough, which is useful for numerical computations.

2.2 Blow-up of conventional flows

In order to construct $\mathcal{J}(T)$, we need to solve the gradient flow (2.2) numerically accurately, and thus it is quite important to understand its properties. Here, we would like to point out that the blow-up of solutions is a quite generic phenomenon for nonlinear differential equations. To be specific, let us consider the asymptotic behavior of the gradient flow (2.2) in simple examples, and we will show that the solutions of (2.2) blow up.

The first example is a quartic potential $S(x) = x^4$. One can regard this as a prototype of the scalar ϕ^4 field theory when the fields are quite large and the mass term is negligible. The gradient flow (2.2) is

$$\frac{dx}{dt} = 4x^3, \quad (2.13)$$

where we consider the case x is real. We can solve this equation with the initial condition $x(0) = x_0 > 0$ as

$$x(t, x_0) = \frac{1}{\sqrt{x_0^{-2} - 8t}}. \quad (2.14)$$

We can readily see that $x(t) \rightarrow \infty$ as $t \nearrow \frac{1}{8x_0^2}$, and the solution blows up within a finite time even for this simple example. One must be careful with the treatment of blow-up when we apply the conventional gradient flow to construct Lefschetz thimbles numerically. Let us make it clear that this is quite a generic phenomenon. For that purpose, we set $k = \deg(S)$, then the flow equation for $r^2 = \sum_i |z^i|^2 (\rightarrow \infty)$ behaves as

$$\frac{dr}{dt} \sim cr^{k-1}, \quad (2.15)$$

with some positive coefficient c . The qualitative behavior is hence given by $r \sim (t_c - t)^{-1/(k-2)}$ for some blow-up time t_c . The only exception is the case when $k = 2$; the blow-up does not occur only if S is Gaussian.

In order to avoid confusion, we emphasize that the blow-up does *not* violate the identity (2.12) if the equations are interpreted appropriately. Returning to the example Eq. (2.13), we now fix the flow time T , and regard $x(T, x_0)$ as a function of the initial condition x_0 in the following way;

$$x(T, x_0) = \begin{cases} +\infty, & x_0 > 1/\sqrt{8T}, \\ x_0/\sqrt{1-8Tx_0^2}, & -1/\sqrt{8T} < x_0 < 1/\sqrt{8T}, \\ -\infty, & x_0 < -1/\sqrt{8T}. \end{cases} \quad (2.16)$$

In this example, the formula (2.12) must be interpreted as

$$Z = \int_{-1/\sqrt{8T}}^{1/\sqrt{8T}} dx_0 \frac{\partial x(T, x_0)}{\partial x_0} \exp[-x(T, x_0)^4], \quad (2.17)$$

which is true since it is obtained by change of variables. In this sense, (2.12) gives the correct answer.

Let us give a heuristic argument why the formula holds true even with the blow-up. As we have seen, $\text{Re}(S(z))$ increases monotonically as the flow time becomes larger. Therefore, as the solution blows up, $\text{Re}(S(z))$ diverges to $+\infty$, which implies that

$$e^{-S(z)} \rightarrow 0. \quad (2.18)$$

The region where the solution blows up within the flow time T does not contribute because the Boltzmann weight vanishes.¹ The rest in the original integration cycle, $(-1/\sqrt{8T}, 1/\sqrt{8T})$, covers the whole $\mathcal{J}(T) \subset \mathbb{C}^n$, which gives the same value as the original integral. Therefore, the blow-up is not the problem of the formulation but requires a correct treatment in numerical computations.

Next, let us consider the following example,

$$Z = \int_{\mathbb{R}} dx (1 - x^2) \exp(-x^2), \quad (2.19)$$

i.e., $S(x) = x^2 - \ln(1 - x^2)$. Here, one can think of factor $(1 - x^2)$ as a toy fermion determinant. We will apply Lefschetz-thimble method to this case, and find that Lefschetz thimbles terminate not only at infinities of the configuration space but also at the zeros of the fermion determinant [19, 20]. In this example, there are no infinities, so let us consider the behavior near zeros of the fermion determinant and set $x = 1 + \delta x$ and $|\delta x| \ll 1$. The conventional flow equation for δx is

$$\frac{d\delta x}{dt} = -\frac{1}{\delta x} + \dots. \quad (2.20)$$

Here, the ellipsis represents the nonsingular terms at $\delta x = 0$, and we neglect them. The solution with the initial condition $\delta x(0) = \delta x_0 \ll 1$ is given by

$$\delta x(t) = \delta x_0 \sqrt{1 - \frac{2t}{\delta x_0^2}}, \quad (2.21)$$

and the flow again reaches the singular point $\delta x = 0$ (or $x = 1$) within the finite time $t = \frac{1}{2}\delta x_0^2$. To interpret the formula (2.12) correctly, at flow time T we must exclude the region $[-1 - \sqrt{2T}, -1 + \sqrt{2T}] \cup [1 - \sqrt{2T}, 1 + \sqrt{2T}]$ from the integral by noticing that $\text{Re}(S) = +\infty$ in this region.²

3 Proposal of new gradient flows without blow-up

In Sec. 2.2, we have seen that the blow-up of conventional gradient flows happens even for very simple examples. The formula for the Lefschetz-thimble integral is still correct

¹Strictly speaking, the discussion given here is slightly imprecise. When the flow blows up, the Jacobian factor $\det(\partial z(T, x)/\partial x)$ diverges. Therefore, the suppression (2.18) must be strong enough to ensure that $\det(\partial z(T, x)/\partial x)e^{-S} \rightarrow 0$. Here we just point out that this is the case for $S(x) = x^4$.

²In the case of the bosonic action, we need require that $\det(\partial z(T, x)/\partial x)e^{-S} \rightarrow 0$. In the fermionic case, this requirement is too strong and not necessarily satisfied. It is enough to require that $\det(\partial z(T, x)/\partial x)e^{-S}$ is bounded around zeros of the fermion determinant because the region with blow-ups shrinks to a set of measure zero. This is actually the case for $S(x) = x^2 - \ln(1 - x^2)$ since the region $[1 - \sqrt{2T}, 1 + \sqrt{2T}]$ shrinks to the point $\{1\}$ while $\det(\partial z(T, x)/\partial x)e^{-S}$ remains finite.

even when blow-up occurs, but we must carefully control that behavior when we perform numerical computations. In this section, we propose a new gradient flow,

$$\frac{dz^i}{dt} = e^{-2\text{Re}(S_B(z))/\Lambda_B} \frac{|D|^2}{|D|^2 + \Lambda_F^{-2}} \overline{\left(\frac{\partial S(z)}{\partial z^i} \right)}, \quad (3.1)$$

for some regularization parameters $\Lambda_B, \Lambda_F \geq 1$. We here consider the case $S(z) = S_B(z) - \ln D(z)$, where $S_B(z)$ is a polynomial that mimics the bosonic action and $D(z)$ is a polynomial that mimics the fermion determinant (i.e., $S_F = -\ln D$ is the effective action for fermions).

3.1 Justification of new gradient flows

In this section, we argue that the new gradient flow (3.1) also defines the Lefschetz-thimble decomposition. To make the argument applicable to more general cases, let us consider a regular Hermitian metric³ $ds^2 = g_{i\bar{j}}(z, \bar{z}) dz^i \otimes d\bar{z}^{\bar{j}}$. Especially, it should be noticed that

$$g_{i\bar{j}}(z, \bar{z}) v^i v^{\bar{j}} > 0 \quad (3.2)$$

for any $z \in \mathbb{C}^n$ and $v \in T_z \mathbb{C}^n \setminus \{0\}$. Using the Hermitian metric, we define the gradient flow as

$$\frac{dz^i}{dt} = g^{i\bar{j}}(z, \bar{z}) \overline{\left(\frac{\partial S(z)}{\partial z^j} \right)}. \quad (3.3)$$

Here, $g^{i\bar{j}}$ is the inverse of metric $g_{i\bar{j}}$. We obtain (3.1) by setting

$$g^{i\bar{j}}(z, \bar{z}) = e^{-2\text{Re}(S_B(z))/\Lambda_B} \frac{|D|^2}{|D|^2 + \Lambda_F^{-2}} \delta^{i\bar{j}}. \quad (3.4)$$

One can easily check that this metric is Hermitian on $\mathbb{C}^n \setminus \{D = 0\}$.

We point out that any choice of the Hermitian metric defines an equivalent Lefschetz-thimble decomposition of the exponential integral. Using the flow equation (3.3), we obtain

$$\frac{dS(z)}{dt} = \frac{\partial S}{\partial z^i} \frac{dz^i}{dt} = g^{i\bar{j}} \frac{\partial S}{\partial z^i} \overline{\frac{\partial S}{\partial z^j}} \geq 0. \quad (3.5)$$

Therefore, the two most important properties of the conventional flow equation are satisfied in the general case (3.3): (a) $\text{Re}(S(z))$ increases monotonically and stays constant only at saddle points, $\partial S(z_\sigma) = 0$. (b) $\text{Im}(S(z))$ is constant along the gradient flow. In Appendix A we will give a proof that all gradient flows define an equivalent Lefschetz thimble decomposition under certain conditions on $S(z)$.

It would be more convincing to relate the new gradient flows (3.1) with the conventional gradient flow. We have introduced two positive parameters Λ_B and Λ_F in the metric of

³In Refs. [40, 41], the Kähler nature of the complexified space is emphasized, but our proposal does not necessarily satisfy the Kähler condition. If one tries to define the intersection number between \mathcal{J}_σ and \mathcal{K}_τ when S has a continuous symmetry, the Kähler nature becomes important to ensure its well-definedness (see Appendix C for more details). Following the recent proposal in Ref. [30], however, one can deform the contour appropriately without using intersection numbers, and thus the Hermitian property would be sufficient for our purpose.

the gradient flow (3.1), and we can obtain the conventional flow equation by taking the limit $\Lambda_B, \Lambda_F \rightarrow \infty$. In this sense, the new and conventional gradient flows are related by a continuous deformation without violating the most important properties of the conventional flow: $\frac{d}{dt}\text{Re}(S) \geq 0$ and $\frac{d}{dt}\text{Im}(S) = 0$ for any $\Lambda_B, \Lambda_F \geq 1$. Let us emphasize that our proposal is just a single example among the huge set of possibilities for the choice of $g^{i\bar{j}}$. Other choices, such as

$$g^{i\bar{j}} = \frac{|D|^2}{(1 + \text{Re}(S_B)^2/\Lambda_B^2)(|D|^2 + \Lambda_F^{-2})} \delta^{i\bar{j}}, \quad (3.6)$$

also satisfy all the above arguments, and we shall show that both choices work nicely to prevent blow-up in finite time.

3.2 Proof of the absence of blow-up

Let us check that the new gradient flows (3.1) *does not* blow up within a finite time. We assume that the action takes the form $S = S_B - \ln D$.

We should notice that the flow diverges along the direction $\text{Re}(S(z)) \rightarrow +\infty$ because $\text{Re}(S)$ monotonically increases. There are two possibilities to realize this divergence:

$$\text{Re}(S_B(z)) \rightarrow \infty, \quad (3.7)$$

or

$$D(z) \rightarrow 0. \quad (3.8)$$

In the first case, $|z| \rightarrow \infty$ since we assumed that $S_B(z)$ is polynomial. In the second case, z approaches a zero of D which are located in a bounded region. It is sufficient for our purpose to analyze the gradient flow in these limiting regions.

We first consider the flow defined by (3.1). We can write the equation as

$$\frac{dz^i}{dt} = e^{-2\text{Re}(S_B(z))/\Lambda_B} \frac{|D(z)|^2}{|D|^2 + \Lambda_F^{-2}} \left(\frac{\partial \overline{S_B(z)}}{\partial z^i} - \frac{1}{D(z)} \frac{\partial \overline{D(z)}}{\partial z^i} \right). \quad (3.9)$$

In the limit $\text{Re}(S_B(z)) \rightarrow +\infty$, all factors on the right hand side except for $e^{-2\text{Re}(S_B)}$ shows a polynomial dependence on z or \bar{z} . Since $|z| \gg 1$ in this region, this implies that dz/dt is exponentially small, which means that $z(t) \rightarrow \infty$ only logarithmically. In the other limit $D(z) \rightarrow 0$, we have that $dz/dt \propto D(z)$ neglecting higher order corrections. Let λ be a zero of $D(z)$ and write $D(z) \simeq (z - \lambda)^k$ for some $k \geq 1$, then the second term in (3.9) gives $\frac{d}{dt}|z - \lambda| \sim -|z - \lambda|^{2k-1}$, so that $|z - \lambda| \sim t^{-1/(2k-2)}$ ($|z - \lambda| \sim \exp(-ct)$ for some $c > 0$ when $k = 1$). In both limits, it takes infinitely long time for the flow to reach the singularities.

We next consider the gradient flow with the metric (3.6):

$$\frac{dz^i}{dt} = \frac{|D(z)|^2}{(1 + \text{Re}(S_B(z))^2/\Lambda_B^2)(|D(z)|^2 + \Lambda_F^{-2})} \left(\frac{\partial \overline{S_B(z)}}{\partial z^i} - \frac{1}{D(z)} \frac{\partial \overline{D(z)}}{\partial z^i} \right). \quad (3.10)$$

The same analysis holds for the limits $D(z) \rightarrow 0$, and we again obtain $|z - \lambda| \sim t^{-1/(2k-2)}$ when z is close to a zero λ of $D(z)$. We now consider the case $\text{Re}(S_B) \rightarrow \infty$ as $|z| \rightarrow \infty$.

To be specific, let $S_B(z)$ is a polynomial of order n , then we obtain that $dz/dt \sim 1/z^{n+1}$. Therefore, $|z(t)| \sim t^{1/(n+2)}$ and it again takes an infinitely long time for the flow to diverge.

As a result, we have analytically shown that the blow-up within finite time can be evaded for certain choices of the Hermitian metric $g_{i\bar{j}}$ on the complexified space \mathbb{C}^n , and we have constructed two specific examples in (3.1) and (3.6). Let us give an intuitive explanation of why the blow-up is prevented by introduction of the metric. For both choices, the metric $g^{i\bar{j}}$ becomes quite small if

$$\text{Re}(S_B) \gtrsim \Lambda_B, |D| \lesssim 1/\Lambda_F. \quad (3.11)$$

Until the flow reaches this region, the new gradient flows show qualitatively the same behavior as the conventional one. However, once the flow reaches this region, the metric decelerates the flow sufficiently, and blow-up does not occur at a finite time.

3.3 On the choice of Λ_B and Λ_F

For practical use of our proposal in numerical computations, the appropriate choice of Λ_B and Λ_F is important. Let us write $g^{i\bar{j}} = g\delta^{i\bar{j}}$, then the introduction of the metric effectively changes the discretization time Δt to $g\Delta t$. If one uses the fourth-order Runge-Kutta method for solving the gradient flow, the error is given by $O((g\Delta t)^4)$.

It is quite natural from this point of view to require that $g \lesssim 1$ while solving the flow starting from real configurations. This puts the constraints on Λ_B as

$$\Lambda_B > \left| 2 \min_{x \in \mathbb{R}^n} \text{Re}(S_B(x)) \right|. \quad (3.12)$$

If we know the complex saddle points $\{z_n\}$ that have nonzero intersection numbers, then the flow reaches to the most dominant saddle points with a reasonable flow time by requiring

$$\Lambda_B > \left| 2 \min_n \text{Re}(S_B(z_n)) \right|. \quad (3.13)$$

It seems that there is no constraint for the upper bound of Λ_B , so one can take a sufficiently large Λ_B that satisfies these constraints.

For any Λ_F , the condition $g < 1$ is satisfied, and thus the lower bound is not given by this consideration. There is, however, an upper bound of Λ_F for practical use. Let z_* be a zero of the fermion determinant, and thus $D(z) \simeq D'(z_*)(z - z_*)$. The flow equation (3.1) in the vicinity of $z = z_*$ reduces to

$$\frac{d}{dt}(z - z_*) \simeq -\Lambda_F^2 |D'(z_*)|^2 (z - z_*). \quad (3.14)$$

The solution is given by

$$z - z_* \propto \exp(-\Lambda_F^2 |D'(z_*)|^2 t). \quad (3.15)$$

In order to solve this exponentially fast convergence, we need to require that $\Lambda_F^2 |D'(z_*)|^2 \Delta t \lesssim 1$ with the discretization time step Δt . As a result, we obtain

$$\Lambda_F \lesssim 1/\sqrt{|D'(z_*)|^2 \Delta t}. \quad (3.16)$$

Although it is difficult to evaluate $D'(z_*)$ for realistic theories, the parametric dependence on Δt of the upper bound of Λ_F is obtained in this way.

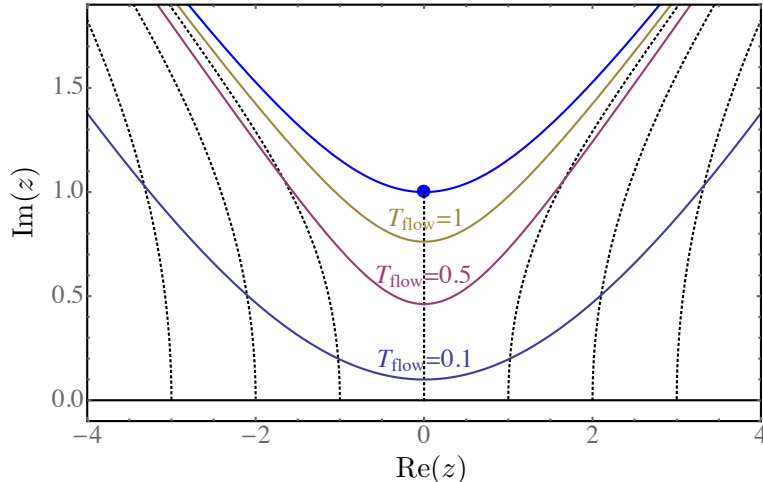


Figure 1. Complex contours $\mathcal{J}_{\Lambda=\infty}(T_{\text{flow}})$ for the Airy integral with the trivial metric. The dashed black curves show flow lines with initial condition at the intersection with the real axis.

4 Numerical tests in simple examples

In this section, we compare behavior of the conventional and new gradient flow numerically for simple examples, the Airy integral, a toy model for a fermion determinant and a one-link U(1) model.

4.1 Airy integral

As a first example, we consider the Airy integration,

$$Z = \text{Ai}(1) = \frac{1}{2\pi} \int_{\mathbb{R}} dx \exp \left\{ i \left(\frac{x^3}{3} + x \right) \right\}. \quad (4.1)$$

The action of this theory is $S(z) = S_B(z) = -i \left(\frac{z^3}{3} + z \right)$, and it has two saddle points at $z = z_{\pm} = \pm i$. The saddle point with non-zero intersection number is $z_+ = i$, and the classical action at that point is $S_B(z_+) = \frac{2}{3}$.

We numerically solve the gradient flow (3.1). Since the fermion determinant is absent, we set $\Lambda_F \rightarrow \infty$ and write $\Lambda = \Lambda_B$:

$$\frac{dz}{dt} = \exp \left(-\frac{2}{\Lambda} \text{Re}(S_B) \right) \overline{\left(\frac{\partial S_B}{\partial z} \right)}. \quad (4.2)$$

The other flows (3.6) give qualitatively similar behaviors, so we do not repeat our analysis. Let $z_{\Lambda}(t, x)$ be the solution with the initial condition $z_{\Lambda}(0, x) = x$, and define the complex contour

$$\mathcal{J}_{\Lambda}(T_{\text{flow}}) = \{z_{\Lambda}(T_{\text{flow}}, x) | x \in \mathbb{R}\}. \quad (4.3)$$

Figure 1 shows the behavior of the gradient flow using the trivial metric, i.e. $\Lambda = \infty$. The solid blue line is the Lefschetz thimble. The dashed lines show the flow lines starting from some real points, and other solid lines show the contours $\mathcal{J}_{\Lambda=\infty}(T_{\text{flow}})$ at $T_{\text{flow}} =$

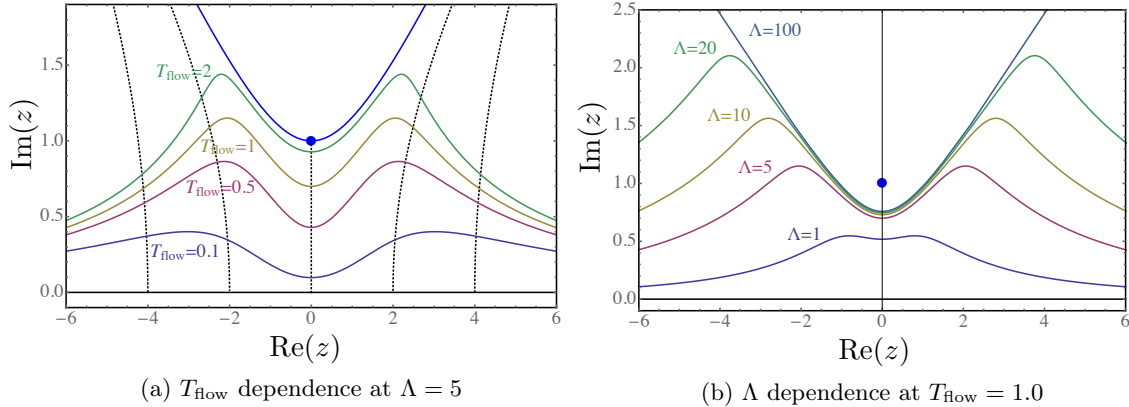


Figure 2. Complex contours $\mathcal{J}_\Lambda(T_{\text{flow}})$ for the Airy integral. The black dashed curves in the left figure show flow lines with initial condition at the intersection with the real axis. The saddle point is denoted by the blue dot which is intersected by the Lefschetz thimble in the left figure.

0.1, 0.5, and 1.0. In Fig. 2, we compute $\mathcal{J}_\Lambda(T_{\text{flow}})$ at several T_{flow} and Λ using fourth-order Runge-Kutta method with time step $\Delta t = 0.001$. We show the T_{flow} -dependence of $\mathcal{J}_\Lambda(T_{\text{flow}})$ at $\Lambda = 5$ in Fig. 2a by computing at $T_{\text{flow}} = 0.1, 0.5, 1.0,$ and 2.0 . In Fig. 2b, we show the Λ -dependence at $T_{\text{flow}} = 1.0$. As we have shown in Sec. 3, the flow equation for any Λ prevents the blow-up since the flow slows down if $\text{Re}(S_B) \gtrsim \Lambda$. Since $S_B(z_+)$ is of the order of 1, we observe in Fig. 2b that $\Lambda = 1$ regularizes the flow too much and the flow stops before reaching the relevant saddle point. For $\Lambda \gtrsim 5$, $\mathcal{J}_\Lambda(T_{\text{flow}} = 1.0)$ almost reaches the saddle point z_+ .

Let us now define the reweighting factor for phase quenching on $\mathcal{J}_\Lambda(T_{\text{flow}})$ by

$$R = \frac{\int_{\mathcal{J}_\Lambda(T_{\text{flow}})} dz \exp(-S(z))}{\int_{\mathcal{J}_\Lambda(T_{\text{flow}})} |dz \exp(-S(z))|} = \frac{\int_{\mathbb{R}} dx \partial_x z_\Lambda(T_{\text{flow}}, x) \exp\{-S(z(T_{\text{flow}}, x))\}}{\int_{\mathbb{R}} dx |\partial_x z_\Lambda(T_{\text{flow}}, x) \exp\{-S(z(T_{\text{flow}}, x))\}|}. \quad (4.4)$$

When $T_{\text{flow}} = 0$, then $\mathcal{J}_\Lambda(0) = \mathbb{R}$ and this reweighting factor vanishes for the Airy integral, $R(T_{\text{flow}}) = 0$. In order to get a better understanding of the qualitative behavior of R , let us comment on the semiclassical evaluation of R in the Lefschetz-thimble method. In this case, only the Lefschetz thimble at $z = z_+$ contributes. Therefore,

$$R(T_{\text{flow}} \rightarrow \infty) \simeq \frac{\sqrt{1/S''(z_+)} e^{-S(z_+)}}{\left| \sqrt{1/S''(z_+)} e^{-S(z_+)} \right|} = 1 \quad (4.5)$$

in the semiclassical approximation, and we expect that R becomes slightly smaller in the exact computation due to the residual sign problem coming from the Jacobian factor $\frac{\partial z_\Lambda(T_{\text{flow}}, x)}{\partial x}$. In Fig. 3, we show the dependence of the reweighting factor on T_{flow} between $0 < T_{\text{flow}} \leq 2.0$ at $\Lambda = 1, 2, 5,$ and 100 . In all cases, R grows monotonically as T_{flow} becomes larger. Since the choice $\Lambda = 1$ regularizes the flow too much as we have discussed, R is not saturated for $T_{\text{flow}} \leq 2.0$. When $\Lambda \gtrsim 5$ for the Airy integral, the additional factor $e^{-2\text{Re}(S_B)/\Lambda}$ in the flow equation decelerates the flow only inside unimportant complex domains, and R shows dependence on Λ very weakly.

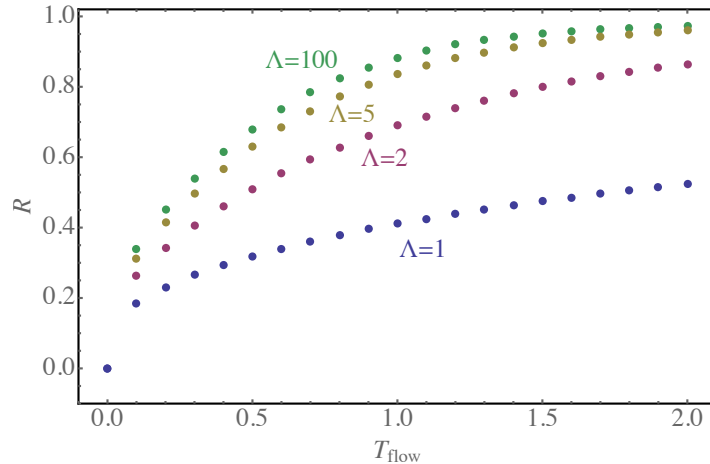


Figure 3. T_{flow} -dependence of the reweighting factor for the Airy integral at various Λ 's.

4.2 Gaussian model with fermion determinant

We consider the following Gaussian integral:

$$Z = \int_{\mathbb{R}} dx (x + i(\alpha - \beta))^p \exp\left(-\frac{1}{2}(x - i\beta)^2\right). \quad (4.6)$$

In this model, the bosonic action is $S_B(z) = \frac{1}{2}(z - i\beta)^2$ and the fermionic determinant is $D(z) = (z + i(\alpha - \beta))^p$, so this model is a prototype of the sign problem with the fermion determinant. Properties of the sign problem of this model (at $\beta = 0$) have been studied with the complex Langevin method in Ref. [65]. The saddle points of the action $S = S_B - \ln D$ are given by

$$z = z_{\pm} = i\beta + \frac{-i\alpha \pm \sqrt{4p - \alpha^2}}{2}. \quad (4.7)$$

For $\alpha < 2\sqrt{p}$, which we refer to as case 1, both the saddle points contribute to the integral, and the complex Langevin method breaks down in generic cases [65]. This failure can be understood as a result of different complex phases for those two Lefschetz thimbles (at least within the semiclassical regime) [29], which necessarily requires a polynomial tail of the complex Langevin distribution and violates assumptions in the formal proof of the complex Langevin method [65–68] (see also Refs. [69, 70] for recent related analytical studies). For $\alpha > 2\sqrt{p}$, both classical solutions are purely imaginary, and only one of the saddle points has non-zero intersection number. In this case, which we refer to as case 2, the complex Langevin method works [65].

4.2.1 Case 1

In the following, we set $p = 2$, $\alpha = 2$, and $\beta = 3$ so that $\alpha^2 < 4p$:

$$z_{\pm} = \pm 1 + 2i. \quad (4.8)$$

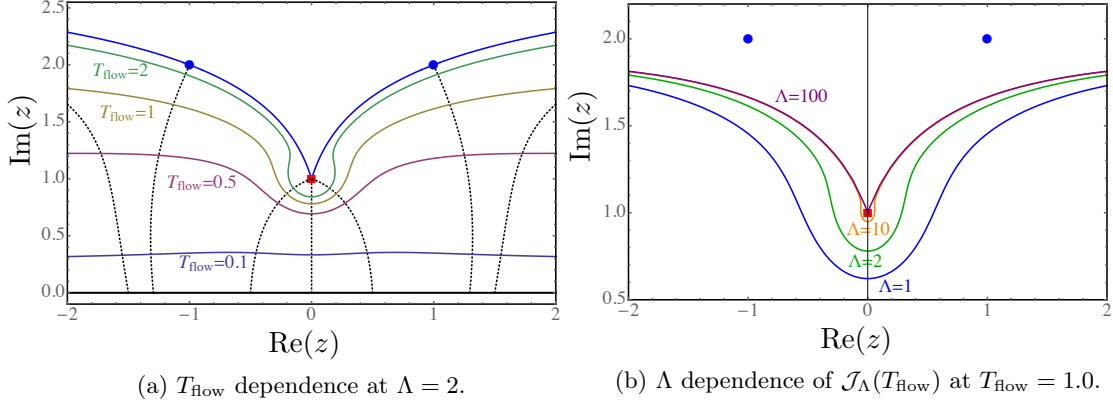


Figure 4. Complex contours $\mathcal{J}_\Lambda(T_{\text{flow}})$ for the Gaussian model with the fermion determinant with $p = 2$, $\alpha = 2$, and $\beta = 3$ (Case 1). The black dashed curves (left figure) show flow lines with initial condition at the intersection with the real axis. The zero of the “fermion determinant” is denoted by the red square while the blue dots shows the saddle points which are intersected by the Lefschetz thimble in the left figure.

The zero of the fermion determinant is located at $z_* = i(\beta - \alpha) = i$. The values of the classical action at $z = z_\pm$ are

$$S(z_\pm) = -\ln(2) \mp \left(1 + \frac{\pi}{2}\right) i. \quad (4.9)$$

We see from this expression that the two saddle points indeed have different phases.

Since the Gaussian bosonic action $S_B = \frac{1}{2}(x - i\beta)^2$ does not cause the blow-up, we set $\Lambda_B \rightarrow \infty$ and concentrate studying the effect of the fermion determinant. We write $\Lambda = \Lambda_F$, and the flow equation becomes

$$\frac{dz}{dt} = \frac{|D(z)|^2}{|D(z)|^2 + \Lambda^{-2}} \left(\frac{\partial \overline{S_B(z)}}{\partial z^i} - \frac{1}{D(z)} \frac{\partial \overline{D(z)}}{\partial z^i} \right). \quad (4.10)$$

We again solve this gradient flow for various Λ using the fourth-order Runge-Kutta method with the time step $\Delta t = 0.01$, and obtain $\mathcal{J}_\Lambda(T_{\text{flow}})$.

In Fig. 4, we show how $\mathcal{J}_\Lambda(T_{\text{flow}})$ develops as T_{flow} and Λ are changed. In Fig. 4a, its T_{flow} -dependence at $\Lambda = 2$ is shown, and $\mathcal{J}_\Lambda(T_{\text{flow}})$ approaches to the saddle point, $z_\pm = \pm 1 + 2i$ as T_{flow} becomes larger. Let us also pay attention to the behavior of flows in the vicinity of the zero of D , $z_* = i$. Since the flow slows down around $z = z_*$, the complex contours $\mathcal{J}_\Lambda(T_{\text{flow}})$ make a slight detour to evade that point. This feature can be more clearly seen by looking at the Λ -dependence of the contours. In Fig. 4b, the Λ -dependence is studied at $T_{\text{flow}} = 1.0$, and the detour becomes smaller as Λ becomes larger. This is consistent with the previous analysis that the flow decelerates if $|D| \lesssim \Lambda^{-1}$.

Figure 5 shows the T_{flow} -dependence of the reweighting factor R at $\Lambda = 1, 2$, and 100 for $0 < T_{\text{flow}} \leq 2.0$. Since the partition function Z is negative with our setup, the reweighting factor R is also negative in this case. The reweighting factor of the conventional phase quenching, i.e. $R(T_{\text{flow}} = 0)$, is about -1.7×10^{-2} when $p = 2$, $\alpha = 2$, and $\beta = 3$, and we can observe how R develops as T_{flow} becomes larger for various values of Λ . To get a

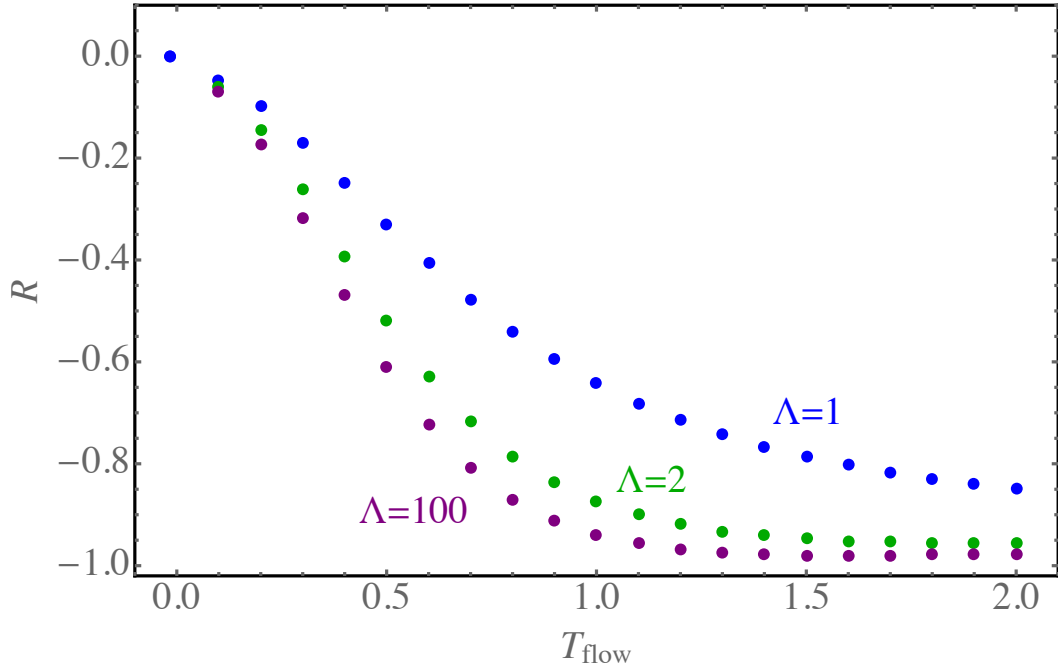


Figure 5. T_{flow} -dependence of the reweighting factor at various Λ 's for the Gaussian model for $p = 2$, $\alpha = 2$, and $\beta = 3$ (Case 1).

better understanding of the figure, let us comment on the semiclassical evaluation of the reweighting factor in the Lefschetz-thimble method. In the saddle-point approximation, the reweighting factor is given by

$$R(T_{\text{flow}} \rightarrow \infty) \simeq \frac{\sqrt{1/S''(z_+)}e^{-S(z_+)} + \sqrt{1/S''(z_-)}e^{-S(z_-)}}{\left| \sqrt{1/S''(z_+)}e^{-S(z_+)} \right| + \left| \sqrt{1/S''(z_-)}e^{-S(z_-)} \right|}. \quad (4.11)$$

It is easy to find that $\sqrt{1/S''(z_{\pm})}e^{-S(z_{\pm})} = c \exp(\pm i(1 + \frac{\pi}{2} + \frac{\pi}{8}))$ for some $c > 0$. As a result, we get $R(T_{\text{flow}} \rightarrow \infty) = \cos(1 + \frac{\pi}{2} + \frac{\pi}{8}) \simeq -0.98$ in the semiclassical approximation, which is roughly consistent with the saturation value given in Fig. 5.

4.2.2 Case 2

In the following, we set $p = 2$, $\alpha = 3$, and $\beta = 4$ so that $\alpha^2 > 4p$, and the saddle points are located at

$$z_+ = 3i, \quad z_- = 2i. \quad (4.12)$$

The zero of the fermion determinant is at $z = z_* = i$. The values of the classical action at $z = z_{\pm}$ are

$$S(z_+) = -\frac{1}{2} - 2 \ln(2) - i\pi, \quad S(z_-) = -2 - i\pi. \quad (4.13)$$

These two classical actions have the same imaginary part, and the theory is indeed on the Stokes ray; two saddle points z_{\pm} are connected by the gradient flow. We again consider the gradient flow given by (4.10).

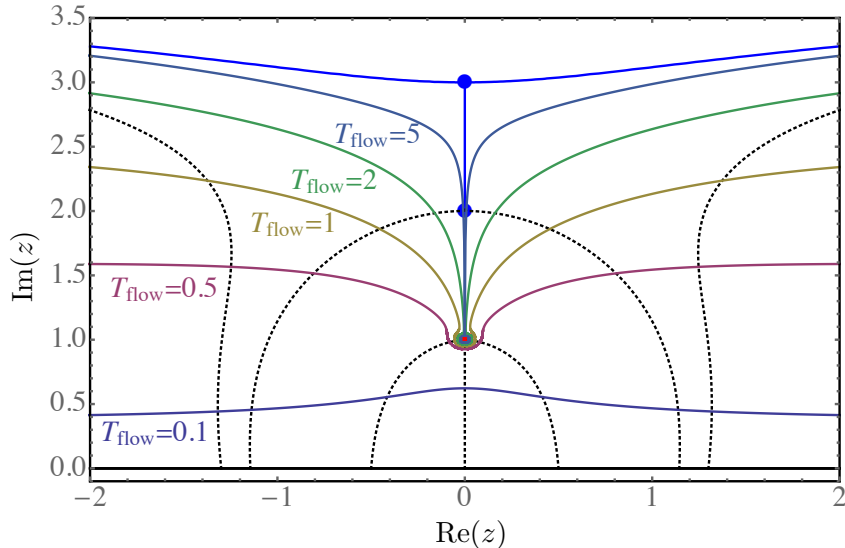


Figure 6. Complex contours $\mathcal{J}_\Lambda(T_{\text{flow}})$ for the Gaussian model with the fermion determinant with $p = 2$, $\alpha = 3$, and $\beta = 4$ (case 2). The saddle points are again denoted by the blue dots with the saddle point at $3i$ intersected by the Lefschetz thimble. The zero of the fermion determinant at i is represented by the red square. The black dashed curves show flow lines with initial condition at the intersection with the real axis.

This is a tricky example because $\mathcal{J}_\Lambda(T_{\text{flow}})$ does not converge to the contributing Lefschetz thimble \mathcal{J}_+ although their homology classes are the same, $[\mathcal{J}_\Lambda(T_{\text{flow}})] = [\mathcal{J}_+]$ (\mathcal{J}_\pm are Lefschetz thimbles associated with saddle points z_\pm). To make the discussion on the intersection number well-defined, let us imagine that we add an infinitesimal imaginary part to parameters α , β so that the theory is off the Stokes ray. If one draws the dual thimbles \mathcal{K}_+ and \mathcal{K}_- , one will find that \mathcal{K}_+ intersects with \mathbb{R} only once but that \mathcal{K}_- intersects with \mathbb{R} twice with different relative orientations. Their intersection number with \mathbb{R} can be computed as $\langle \mathbb{R}, \mathcal{K}_+ \rangle = 1$ and $\langle \mathbb{R}, \mathcal{K}_- \rangle = 1 - 1 (= 0)$. As a result, the Lefschetz-thimble decomposition of the integral becomes

$$\int_{\mathbb{R}} dx \exp(-S(x)) = \int_{\mathcal{J}_+ + \mathcal{J}_- - \mathcal{J}_-} dz \exp(-S(z)) = \int_{\mathcal{J}_+} dz \exp(-S(z)). \quad (4.14)$$

We can now see why $\mathcal{J}_\Lambda(T_{\text{flow}}) \not\rightarrow \mathcal{J}_+$ as $T_{\text{flow}} \rightarrow \infty$ as manifolds: The construction of $\mathcal{J}_\Lambda(T_{\text{flow}})$ is sensitive to the cancellation of two intersections between \mathcal{K}_- and \mathbb{R} , and thus the limit of $\mathcal{J}_\Lambda(T_{\text{flow}})$ roughly becomes

$$\lim_{T_{\text{flow}} \rightarrow \infty} \mathcal{J}_\Lambda(T_{\text{flow}}) \simeq (-\infty + z_+, z_+ - 0^+) \cup [z_+ - 0^+, z_*] \cup [z_*, z_+ + 0^+] \cup [z_+ + 0^+, z_+ + \infty). \quad (4.15)$$

Since $\mathcal{J}_+ \simeq (-\infty + z_+, z_+ + \infty)$, there are additional line segments, along which the integrals of holomorphic functions cancel. This observation is important when we discuss the reweighting factor, since the additional segments reduce the reweighting factor: $R(T_{\text{flow}} \rightarrow \infty) \simeq -0.45$.

Since the Λ dependence is quite weak except in the vicinity of $z = z_* = i$ for $\Lambda \gtrsim 10$ as we have seen in Fig. 4b for slightly different parameters, let us show the numerical result

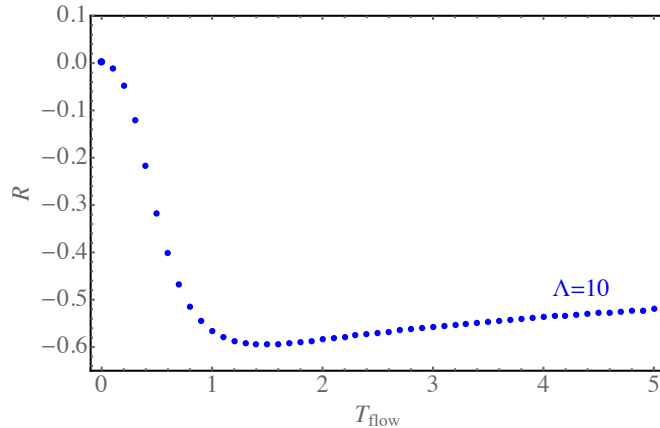


Figure 7. T_{flow} -dependence of the reweighting factor at $\Lambda = 10$ for the Gaussian model for $p = 2$, $\alpha = 3$, and $\beta = 4$.

only at $\Lambda = 10$. Figure 6 gives the T_{flow} dependence of contours $\mathcal{J}_\Lambda(T_{\text{flow}})$ at $\Lambda = 10$ for $0 < T_{\text{flow}} \leq 5.0$. We find that $\mathcal{J}_\Lambda(T_{\text{flow}})$ indeed approaches the contour given in (4.15) as T_{flow} gets larger. Moreover, thanks to the metric in the gradient flow, $\mathcal{J}_\Lambda(T_{\text{flow}})$ detours evading the zero of the fermion determinant $z = z_*$.

Figure 7 shows the T_{flow} dependence of the reweighting factor. Interestingly, the reweighting factor reaches the maximum around $T_{\text{flow}} \simeq 1.4$ and overcomes the reweighting factor, $R(T_{\text{flow}} \rightarrow \infty) \simeq -0.45$, computed by using Lefschetz thimbles. It gradually decreases after that, and approaches to $R(T_{\text{flow}} \rightarrow \infty) \simeq -0.45$.

4.3 $U(1)$ one-link model

The $U(1)$ one-link model is given by

$$Z = \int_{-\pi}^{\pi} \frac{dx}{2\pi} e^{\beta \cos(x)} [1 + \kappa \cos(x - i\mu)]. \quad (4.16)$$

The bosonic action is $S_B(z) = -\beta \cos(z)$, and the fermion determinant is given by $D(z) = (1 + \kappa \cos(z - i\mu))$. This model is considered in Ref. [16] in the context of Lefschetz thimbles. In order to control the blow-ups of this model at various values of the parameters, we need to introduce both Λ_B and Λ_F in the metric of the gradient flow. We shall see that our proposal to change the flow works well also for this situation. The structure of Lefschetz thimbles changes drastically as the parameter κ exceeds 1, so we consider the cases $\kappa = 1/2$ and $\kappa = 2$. We always set $\beta = 1$ and $\mu = 2$.

4.3.1 Small κ

We take $\kappa = 1/2$, $\beta = 1$, and $\mu = 2$ in (4.16), and we set $\Lambda_B = 5$ throughout the analysis in this case. The relevant saddle points are approximately given by

$$z_1 \simeq 0.48i, \quad z_2 \simeq \pi + 1.17i. \quad (4.17)$$

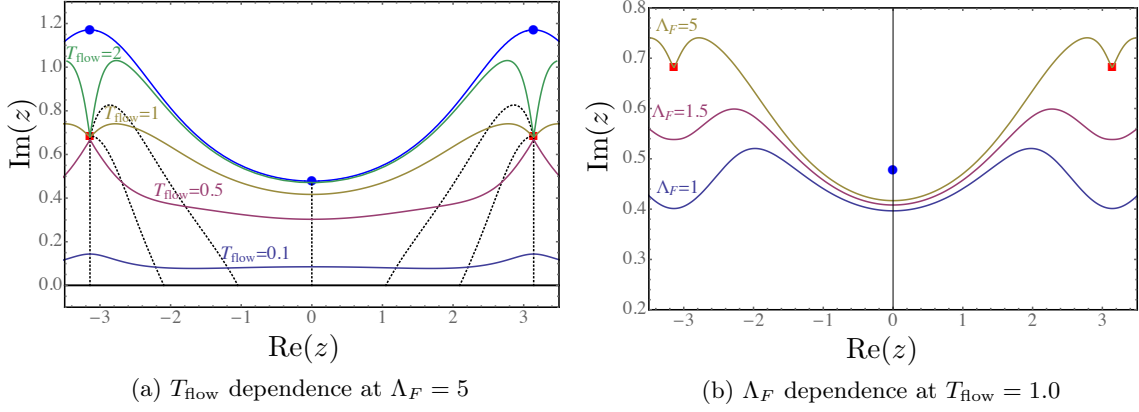


Figure 8. Complex contours $\mathcal{J}_\Lambda(T_{\text{flow}})$ for the $U(1)$ one-link model with $\kappa = 1/2$. We set $\Lambda_B = 5$. The saddle points are denoted by the blue dots while the zeros of the fermion determinant are depicted as red squares. The dashed curves in the left figure are flow lines which end at a zero of the fermion determinant or at the saddle point on the imaginary axis which is intersected by the Lefschetz thimble.

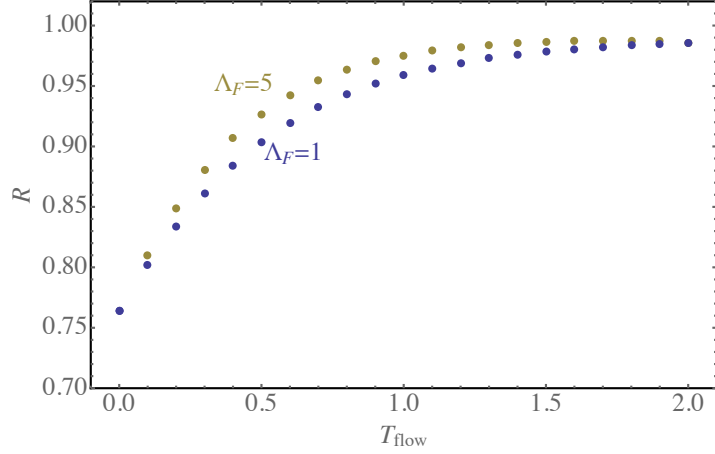


Figure 9. T_{flow} -dependence of the reweighting factor for the $U(1)$ one-link model with $\kappa = 1/2$ and $\Lambda_B = 5$.

The values of the classical action at these saddle points are $S_1 \simeq -1.9$ and $S_2 \simeq 2.9$, respectively, and thus the contribution is dominated by z_1 . The zeros of the fermion determinant are located at

$$z_{*\pm} = \pi + i(\mu \pm \cosh^{-1}(1/\kappa)). \quad (4.18)$$

In Fig. 8a, the blue solid curve shows the Lefschetz thimble of z_1 that contributes to Z , and red squares show the zero z_{*-} of the fermion determinant. We show in Fig. 8a how $\mathcal{J}_\Lambda(T_{\text{flow}})$ develops as T_{flow} increases at $\Lambda_B = \Lambda_F = 5$. In Fig. 8b, the Λ_F dependence of $\mathcal{J}_\Lambda(T_{\text{flow}})$ is studied at $T_{\text{flow}} = 1.0$, and the contours approach to $z = z_{*-}$ as Λ_F becomes larger. In this parameter region, Λ_B does not play a significant role, because the blow-up due to the bosonic action S_B does not occur.

Figure 9 shows the T_{flow} -dependence of the reweighting factor at $\Lambda_F = 1$ and 5. We find

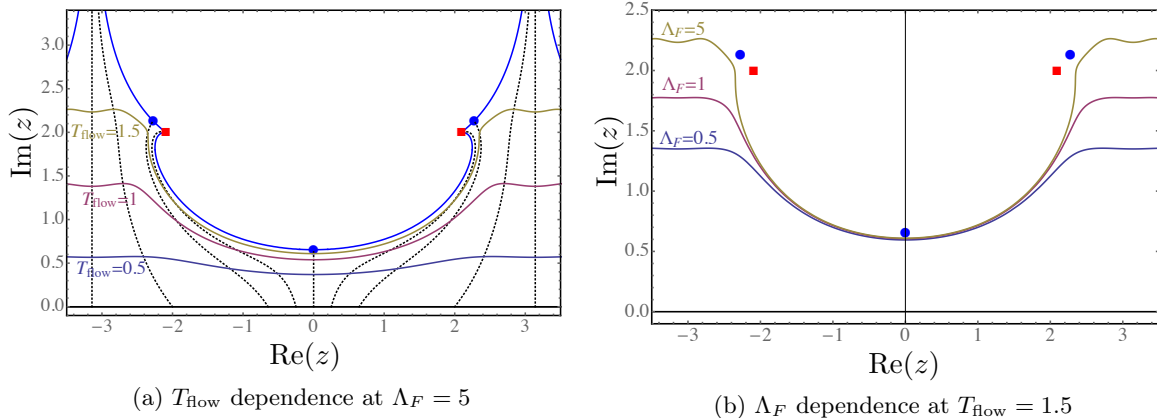


Figure 10. Complex contours $\mathcal{J}_\Lambda(T_{\text{flow}})$ for the $U(1)$ one-link model with $\kappa = 2$. We set $\Lambda_B = 10$. The saddle points, which in the left figure are intersected by the Lefschetz thimble, are denoted by the blue dots while the zero or the fermion determinant are shown as red squares. The dashed black curves show flow lines with initial condition on the real axis.

that the Λ_F dependence of the reweighting factor is quite small even though the contours themselves strongly depend of Λ_F as we have seen in Fig. 8b. In this case, the contribution to Z is dominated by one saddle point z_1 , and thus the reweighting factor becomes close to 1. For $\Lambda_F = 5$, the reweighting factor reaches its maximum around $T_{\text{flow}} \simeq 1.6$, and it slightly decreases after that. This is because the zero z_{*-} obstructs the deformation of real cycle to the Lefschetz thimble shown by the blue solid curve as we have seen in the Gaussian model, and thus the residual sign problem becomes more severe when T_{flow} becomes larger than a certain value.

4.3.2 Large κ

We take $\kappa = 2$, $\beta = 1$, and $\mu = 2$ in (4.16), and we set $\Lambda_B = 10$ throughout the analysis in this case. The relevant saddle points are approximately given by

$$z_1 \simeq 0.65i, \quad z_{2,3} \simeq \pm 2.28 + 2.13i. \quad (4.19)$$

The values of the classical action at these saddle points are $S_1 \simeq -2.9$ and $S_{2,3} \simeq 3.8 \pm 5.7i$, and thus the contribution is dominated by z_1 . The zeros of the fermion determinant are given by

$$z_{*\pm} = \pm(\pi - \cos^{-1}(1/\kappa)) + i\mu. \quad (4.20)$$

These zeros are shown with red squares in Fig. 10a, and the blue solid curves show the Lefschetz thimbles contributing to Z .

In Fig. 10a we study the T_{flow} -dependence of $\mathcal{J}_\Lambda(T_{\text{flow}})$ at $\Lambda_F = 5$. In this case, Λ_B prevents the blow-up in the direction $z \rightarrow \pi + i\infty$. The Λ_F -dependence of $\mathcal{J}_\Lambda(T_{\text{flow}})$ is studied in Fig. 10b, and the contour becomes similar to Lefschetz thimbles as Λ_F becomes larger.

Figure 11 shows the T_{flow} -dependence of the reweighting factor at $\Lambda_F = 0.5$ and 5. The Λ_F -dependence of the reweighting factor is quite small. Within the time interval in our

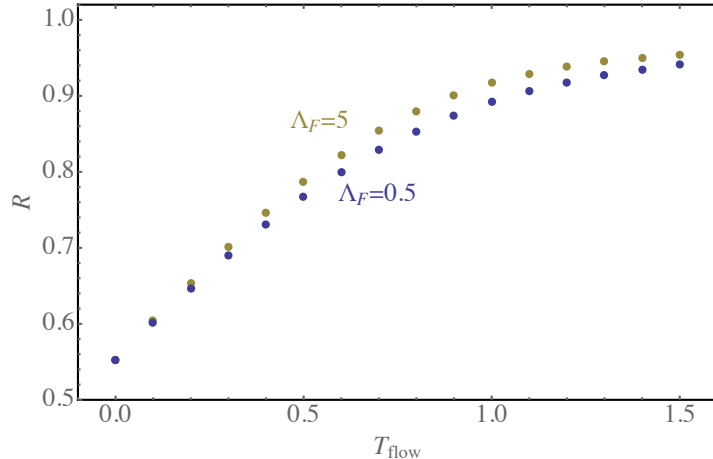


Figure 11. T_{flow} -dependence of the reweighting factor for the $U(1)$ one-link model with $\kappa = 2$ and $\Lambda_B = 10$.

computation, the reweighting factor monotonically increases for this parameter. Compared with other examples studied in this paper, this model is an important benchmark because both Λ_B and Λ_F are effective to prevent the blow-up in this parameter region. We have checked through this model that the reweighting factor behaves as we have expected even in such situations.

5 Conclusions

We have argued that the conventional gradient flow defining Lefschetz thimbles generically blows up, and thus one needs to monitor the divergence of gradient flows with great care in numerical computations. Instead of doing that, we propose a new gradient flow equation (3.1) that also defines Lefschetz thimbles and does not suffer from blow-ups. We show its theoretical foundation by providing a geometric interpretation of the change in the gradient flows, and also prove rigorously that our new flow equation does not have blow-ups. In some examples of one-dimensional integrals with a sign problem, we numerically construct the complex contours using the new gradient flow to see how it works in practice. By appropriately choosing the regularization parameters of the new gradient flow, we check that it solves the sign problem as the conventional flow equation does.

One possible concern about our proposal would be the numerical cost, but we believe that it is not the problem for the following reasons. Since the computation of the metric needs the absolute value of the fermion determinant, it takes $O(N^3)$ in the LU decomposition when N is the size of the fermion matrix. However, one needs to compute the inverse of the fermion matrix even without introducing the metric and it also costs $O(N^3)$, so this additional computational cost would not be a severe problem. Moreover, if the precise evaluation of the determinant is too costly, we could use the stochastic estimation of the determinant that reduces the cost significantly.

Let us also briefly discuss another possible remedy treating the blow-up and compare it with our proposal. A simple remedy that uses the conventional flow equation would be the

following: Introducing a cutoff in the process of solving the conventional flow equation in order to estimate the blow-up, we throw away a trial configuration when it satisfies a preset blow-up criterion. The argument is that blow-up occurs when the action diverges and such configurations are suppressed anyway. However, for strongly-coupled field theories, the configurations with exponentially small Boltzmann weights can give a significant contribution because of the exponentially large entropy, and we must check the cutoff-independence of the results obtained using this simple remedy. In our proposal, although additional costs are required to compute the metric, we do not introduce any cutoffs in doing the Monte Carlo algorithm. Since the additional computational costs for the metric is at most the same order of the computation for original flow equations, the check of cutoff-independence and our proposal would be comparable. Another possible merit for introducing the metric is that the flow equations becomes more stable than the original ones because of the absence of a blow-up, which allows to increase the step-size of the flow equation reducing the computational cost.

Our proposal (3.1) is only one possible way to introduce a metric in the gradient flow that prevents blow-up. We have shown that other choices define an equivalent Lefschetz-thimble decomposition so long as the gradient flow takes the form (3.3). We therefore would like to comment that technical problems of solving gradient flow equations might be circumvented by choosing a different metric.

It would be interesting to see how our proposal works for the path integral of more realistic systems with strong interaction. Toward the final goal of computing finite-density QCD, chiral random matrix is a good candidate to be tested. Indeed, previous studies [71–81] reveal that chiral symmetry breaking and associated charged pions are the origin of the difficulties for the numerical simulations of cold and dense QCD. Since chiral random matrix theory shares the same universality with regards to the Dirac-eigenvalue distributions, its systematic study with Lefschetz thimbles, which is partly done in Ref. [22], will provide us an important insight in this problem.

Acknowledgments

Y. T. thanks Francesco Di Renzo and Giovanni Eruzzi for useful discussions and their kindness at VIII Parma International School of Theoretical Physics. Y. T. and H. N. are financially supported by Special Postdoctoral Researchers program of RIKEN.

A Proof of equivalence among gradient flows

In this Appendix, we prove that the Lefschetz-thimble decompositions with different Hermitian metrics $g_{i\bar{j}}$ are equivalent. We assume that $S(z)$ is a polynomial on \mathbb{C}^n without degenerate critical points and critical points at infinities. We further assume that the $\text{Im}(S(z_\sigma))$ are all different for different saddle points.

We denote the solution of the gradient flow with the metric g as $z^{(g)}(t)$, and define the Lefschetz thimble and its dual by

$$\mathcal{J}_\sigma^{(g)} = \{z^{(g)}(0) \in \mathbb{C}^n \mid z^{(g)}(-\infty) = z_\sigma\}, \quad (\text{A.1})$$

$$\mathcal{K}_\sigma^{(g)} = \{z^{(g)}(0) \in \mathbb{C}^n \mid z^{(g)}(+\infty) = z_\sigma\}. \quad (\text{A.2})$$

We can show that

$$\langle \mathcal{J}_\sigma^{(g)}, \mathcal{K}_\tau^{(g)} \rangle = \delta_{\sigma\tau}. \quad (\text{A.3})$$

This is because $\text{Im}(S(z))$ is constant on each $\mathcal{J}_\sigma^{(g)}$, $\mathcal{K}_\tau^{(g)}$, and hence the above assumption on $\text{Im}(S)$ implies $\mathcal{J}_\sigma^{(g)}$ and $\mathcal{K}_\tau^{(g)}$ cannot intersect when $\sigma \neq \tau$. We should notice that $\mathcal{J}_\sigma^{(g)}$ and $\mathcal{K}_\sigma^{(g)}$ intersects only at z_σ since $\text{Re}(S(z))$ is monotonically increasing along the flow. Moreover, the same argument shows that

$$\langle \mathcal{J}_\sigma^{(g)}, \mathcal{K}_\tau^{(g')} \rangle = \delta_{\sigma\tau} \quad (\text{A.4})$$

even when \mathcal{J} and \mathcal{K} are defined by different metrics g, g' .

Since $\text{Re}(S(z))$ increases monotonically along the gradient flow, $\mathcal{J}^{(g)}$ defines integration cycles of the form $e^{-S(z)} d^n z$. Therefore,

$$[\mathcal{J}_\sigma^{(g)}] \in H_n(\mathbb{C}^n, \{e^{-\text{Re}(S)} \ll 1\}) \simeq \sum_\sigma \mathbb{Z} \mathcal{J}_\sigma. \quad (\text{A.5})$$

Similarly,

$$[\mathcal{K}_\sigma^{(g)}] \in H_n(\mathbb{C}^n, \{e^{-\text{Re}(S)} \gg 1\}) \simeq \sum_\sigma \mathbb{Z} \mathcal{K}_\sigma. \quad (\text{A.6})$$

Using the above property on the intersection pairing, we obtain the identity for the homology class,

$$[\mathcal{J}_\sigma^{(g)}] = \sum_\tau \langle \mathcal{J}_\sigma^{(g)}, \mathcal{K}_\tau \rangle [\mathcal{J}_\tau] = [\mathcal{J}_\sigma]. \quad (\text{A.7})$$

Similarly, we obtain

$$[\mathcal{K}_\sigma^{(g)}] = [\mathcal{K}_\sigma]. \quad (\text{A.8})$$

This shows that the homology class of the Lefschetz thimble does not depend on the choice of Hermitian metric. It also shows that

$$Z = \sum_\sigma \langle \mathbb{R}^n, \mathcal{K}_\sigma \rangle \int_{\mathcal{J}_\sigma^{(g)}} d^n z \exp[-S(z)] \quad (\text{A.9})$$

for any choice of g . Here, we emphasize again that the coefficients $\langle \mathbb{R}^n, \mathcal{K}_\sigma \rangle$ are independent of the choice of metric g . It partly comes from the fact that the intersection number is a topological quantity while the metric is a regular complex function. The intersection number thus jumps only when the Stokes phenomenon happens, and what we have shown here is that the change of the metric does not cause the Stokes jumping.

There are a few remarks on this result. For the one-dimensional examples, the Lefschetz thimble is nothing but the stationary phase contour, that is characterized by $\text{Im}(S(z))$ being constant. Since this amounts to one constraint in the two-dimensional space $\mathbb{C} \simeq \mathbb{R}^2$, the

Lefschetz thimble is uniquely defined as a submanifold. Independence of the metric is trivial since the stationary phase condition does not use the metric. On the other hand, this is highly nontrivial if one considers higher-dimensional integrals. In this case, the stationary phase condition is insufficient to characterize the half-dimensional submanifolds in \mathbb{C}^n , and there are a lot of possible choices for steepest descent cycles. Therefore, \mathcal{J}_σ and $\mathcal{J}_\sigma^{(g)}$ can be different submanifolds of \mathbb{C}^n if $n \geq 2$. Application of the Picard–Lefschetz theory ensures that all of them are “equivalent” in the sense that their homology class is the same.

B Flow equation for the Jacobian matrix

For the numerical computation of the Lefschetz-thimble Monte Carlo method, we do not only need the flow $z(T, x)$ but also the flow of the Jacobian $\det(\partial z^i(T, x)/\partial x^j)$. We first derive the result for the most general expression (3.3), and then apply it to the cases (3.1) and (3.6).

Let us consider two solutions with infinitesimally close initial conditions $z(T, x)$ and $z(T, x + \Delta x)$, where $|\Delta x| \ll 1$. We compute the deviation of the gradient flow (3.3) as

$$\frac{d\Delta z^i}{dt} = \left(g^{i\bar{j}} \partial_{\bar{j}} \partial_{\bar{k}} \bar{S} + \partial_{\bar{k}} g^{i\bar{j}} \partial_{\bar{j}} \bar{S} \right) \overline{\Delta z^k} + \partial_k g^{i\bar{j}} \partial_{\bar{j}} \bar{S} \Delta z^k. \quad (\text{B.1})$$

Here, we introduced the shorthand notation $\partial_i = \partial/\partial z^i$ and $\partial_{\bar{i}} = \partial/\partial \bar{z}^i$, and $\Delta z = z(t, x + \Delta x) - z(t, x)$. By writing the Jacobian matrix by

$$J_j^i(t, x) = \frac{\partial z^i(t, x)}{\partial x^j}, \quad (\text{B.2})$$

Δz becomes $\Delta z^i = J_j^i \Delta x^j$. To compute the Jacobian, we consider a real-valued variation for Δx , and thus we obtain

$$\frac{dJ_\ell^i}{dt} = \left(g^{i\bar{j}} \partial_{\bar{j}} \partial_{\bar{k}} \bar{S} + \partial_{\bar{k}} g^{i\bar{j}} \partial_{\bar{j}} \bar{S} \right) \overline{J_\ell^k} + \partial_k g^{i\bar{j}} \partial_{\bar{j}} \bar{S} J_\ell^k \quad (\text{B.3})$$

by comparing coefficients of Δx^ℓ . If one assumes that $g^{i\bar{j}} \propto \delta^{i\bar{j}}$ at the saddle points $\partial_i S = 0$, then one can solve this equation in the vicinity of a saddle point by applying Takagi’s factorization to $\partial_{\bar{i}} \partial_{\bar{k}} \bar{S}$.

Let us restrict ourselves to diagonal metrics $g^{i\bar{j}}(z, \bar{z}) = g(z, \bar{z}) \delta^{i\bar{j}}$. Then, we obtain

$$\begin{aligned} \frac{dJ_\ell^i}{dt} &= (g \partial_{\bar{i}} \partial_{\bar{k}} \bar{S} + \partial_{\bar{i}} \bar{S} \partial_{\bar{k}} g) \overline{J_\ell^k} + \partial_{\bar{i}} \bar{S} \partial_k g J_\ell^k \\ &= g \left[(\partial_{\bar{i}} \partial_{\bar{k}} \bar{S} + \partial_{\bar{i}} \bar{S} \partial_{\bar{k}} \ln g) \overline{J_\ell^k} + (\partial_{\bar{i}} \bar{S} \partial_k \ln g) J_\ell^k \right]. \end{aligned} \quad (\text{B.4})$$

For the conventional gradient flow (2.2), we reproduce the well-known formula [10]

$$\frac{dJ_\ell^i}{dt} = (\partial_{\bar{i}} \partial_{\bar{k}} \bar{S}) \overline{J_\ell^k} \quad (\text{B.5})$$

by substituting $g = 1$.

For the proposed gradient flow (3.1), we need to compute $\partial_k \ln g$ for the metric (3.4):

$$\partial_k \ln g = -\frac{\partial_k S_B}{\Lambda_B} + \frac{\Lambda_F^{-2} D^{-1} \partial_k D}{|D|^2 + \Lambda_F^{-2}}. \quad (\text{B.6})$$

We obtain $\partial_{\bar{k}} \ln g$ by taking the complex conjugation since g is real. As a result, the deviation equation for (3.1) is given by

$$\begin{aligned} \frac{dJ_\ell^i}{dt} = & e^{-2\text{Re}(S_B)/\Lambda_B} \frac{|D|^2}{|D|^2 + \Lambda_F^{-2}} \left[\left\{ \partial_i \partial_{\bar{k}} \bar{S} + \partial_{\bar{i}} \bar{S} \left(-\frac{\partial_{\bar{k}} \bar{S}_B}{\Lambda_B} + \frac{\bar{D}^{-1} \partial_{\bar{k}} \bar{D}}{\Lambda_F^2 |D|^2 + 1} \right) \right\} \bar{J}_\ell^k \right. \\ & \left. + \left\{ \partial_{\bar{j}} \bar{S} \left(-\frac{\partial_k S_B}{\Lambda_B} + \frac{D^{-1} \partial_k D}{\Lambda_F^2 |D|^2 + 1} \right) \right\} J_\ell^k \right]. \end{aligned} \quad (\text{B.7})$$

C Comment on the Hermitian and Kähler metric in the gradient flow

In the original applications of Lefschetz thimbles to quantum gauge theories [40, 41], the Kähler nature of the complexified field space was emphasized. Our proposal (3.1), however, introduces the Hermitian metric in the gradient flow, and it is not Kähler. In this appendix, we will justify the use of our proposal even for the sign problem of lattice gauge theories.

C.1 Quick review on complex structure

This is the brief summary of Hermitian and Kähler structures. In the following, we consider a $2n$ -dimensional smooth (real) manifold M .

If there exists a bundle map $J : TM \rightarrow TM$ with $J^2 = -1$ and TM the tangent bundle of M , we call J an almost complex structure on M . By considering a complexification of the tangent bundle $TM \otimes_{\mathbb{R}} \mathbb{C}$, one can diagonalize J at each point $p \in M$ with eigenvalues $\pm\sqrt{-1}$ and degeneracies n_{\pm} . If $J = J_\mu^\nu \partial_\nu \otimes dx^\mu$ satisfies the integrability condition,

$$J_\mu^\nu (\partial_\rho J_\sigma^\mu - \partial_\sigma J_\rho^\mu) + J_\sigma^\mu \partial_\mu J_\rho^\nu - J_\rho^\mu \partial_\mu J_\sigma^\nu = 0, \quad (\text{C.1})$$

we say J is a complex structure of M , and M is called a complex manifold.

If M is a complex manifold, we can take local (holomorphic and anti-holomorphic) coordinates z^i and $\bar{z}^{\bar{i}} = \overline{z^i}$ ($i = 1, \dots, n$), which diagonalizes J at each point and the transformation property among them is holomorphic, thanks to Newlander–Nirenberg theorem. More concretely, in such coordinates the complex structure looks like

$$J_i^j = \sqrt{-1} \delta_i^j, \quad J_{\bar{i}}^{\bar{j}} = -\sqrt{-1} \delta_{\bar{i}}^{\bar{j}}, \quad J_i^{\bar{j}} = J_{\bar{i}}^j = 0. \quad (\text{C.2})$$

If one takes another coordinate patch w^i and $\bar{w}^{\bar{i}}$ with the same property, then $w^i(z)$ are holomorphic and $\bar{w}^{\bar{i}}(\bar{z})$ are anti-holomorphic thanks to the integrability condition.

C.1.1 Hermitian structure

A Riemannian manifold with an (almost) complex structure (M, g, J) is called Hermitian if it satisfies

$$g_{\mu\nu} J_\rho^\mu J_\sigma^\nu = g_{\rho\sigma}. \quad (\text{C.3})$$

Let us take a holomorphic local coordinate z^i , then this condition implies

$$(ds)^2 = g_{i\bar{j}}(dz^i \otimes dz^{\bar{j}} + dz^{\bar{j}} \otimes dz^i). \quad (\text{C.4})$$

That is, $g_{ij} = g_{\bar{i}\bar{j}} = 0$. Using the mixed component of the metric, one can define a non-degenerate 2-form, called the Hermitian form,

$$\omega = ig_{i\bar{j}}dz^i \wedge dz^{\bar{j}}. \quad (\text{C.5})$$

C.1.2 Kähler structure

A Riemannian manifold with a complex structure (M, g, J) is called Kähler if it satisfies

- $D_\mu J_\rho^\nu = 0$ (D_μ is the covariant derivative with the Levi-Civita connection),
- $g_{\mu\nu} J_\rho^\mu J_\sigma^\nu = g_{\rho\sigma}$.

Compared to the Hermitian case, the first condition is imposed additionally for the Kähler manifold. Let us take a holomorphic local coordinate z^i again, then the second condition implies that $g_{ij} = g_{\bar{i}\bar{j}} = 0$, i.e.,

$$(ds)^2 = g_{i\bar{j}}(dz^i \otimes dz^{\bar{j}} + dz^{\bar{j}} \otimes dz^i). \quad (\text{C.6})$$

Using the mixed component of the metric, one can define a 2-form, called the Kähler form,

$$\omega = ig_{i\bar{j}}dz^i \wedge dz^{\bar{j}}. \quad (\text{C.7})$$

The first condition means that $\partial_i g_{j\bar{k}} = \partial_j g_{i\bar{k}}$ and $\partial_{\bar{i}} g_{j\bar{k}} = \partial_{\bar{k}} g_{j\bar{i}}$, and it is equivalent to say that ω is symplectic, i.e.,

$$d\omega = 0. \quad (\text{C.8})$$

That is, one can say that Kähler manifolds are Hermitian manifolds whose Hermitian forms are symplectic. This condition ensures the existence of a local function K , which is called a Kähler potential, so that $\omega = i\partial\bar{\partial}K$, where ∂ and $\bar{\partial}$ are holomorphic and anti-holomorphic exterior derivatives (they are called Dolbeault operators, and locally $\partial = dz^i \partial_i$, etc.). Note that K is not necessarily a (globally defined) function, which is why K is called "potential".

C.2 Gradient flow and Hamilton equation of motion

In this section, we first review why the Kähler nature of the complexified space is useful for analytic applications of the Lefschetz-thimble method to topological gauge theories [40, 41]. In the last paragraph, we argue that practical applications do not require the Kähler property, and we will conclude that the Hermitian metric can be used to define the flow equation of lattice gauge theories when treating the sign problem.

Let us pick up a holomorphic map $S : M \rightarrow \mathbb{C}$, and consider the flow equation,

$$\frac{dz^i}{dt} = g^{i\bar{j}} \partial_{\bar{j}} \bar{S}. \quad (\text{C.9})$$

This can be viewed from two perspectives, the Hermitian or the Kähler manifold. From the Riemannian nature of M , this is the gradient flow with the height function $\text{Re}(S) = (S + \bar{S})/2 : M \rightarrow \mathbb{R}$,

$$\frac{dx^\mu}{dt} = g^{\mu\nu} \partial_\nu 2\text{Re}(S). \quad (\text{C.10})$$

One can easily check that in the holomorphic coordinate this goes back to the original equation (C.9) using the Cauchy–Riemann condition. In order to get another perspective, we introduce a “bracket” defined from the Hermitian or Kähler form ω :

$$\{f, g\} = -ig^{i\bar{j}}(\partial_i f \partial_{\bar{j}} g - \partial_i g \partial_{\bar{j}} f). \quad (\text{C.11})$$

If we consider the following equation with $\text{Im}(S) = (S - \bar{S})/(2i) : M \rightarrow \mathbb{R}$,

$$\frac{dx^\mu}{dt} = \{x^\mu, 2\text{Im}(S)\}, \quad (\text{C.12})$$

it again gives the original equation (C.9). Since $\{f, f\} = 0$ in general, this elucidates that $\text{Im}(S)$ is conserved along the flow equation.

The huge merit in choosing the Kähler metric comes from the fact that $\{, \}$ becomes the Poisson bracket for the Kähler form ω , i.e. it satisfies the Jacobi identity $\{f, \{g, h\}\} + \{g, \{h, f\}\} + \{h, \{f, g\}\} = 0$. Therefore, for the Kähler metric, the gradient flow has a classical mechanical interpretation [40, 41].

If $\text{Re}(S)$ is a Morse function on M and satisfies the Morse–Smale condition (i.e., the critical points of S are non-degenerate and with all different $\text{Im}(S)$ at those critical points), then one can compute basis of relative homologies $H_n(M, \{e^{-\text{Re}(S)} \ll 1\})$ and $H_n(M, \{e^{-\text{Re}(S)} \gg 1\})$ using the gradient flow, as we have seen in Appendix A. Those bases are called Lefschetz thimbles and dual thimbles, respectively. There exists a natural pairing called the intersection pairing, and this is important for the decomposition of the middle-dimensional cycles in terms of Lefschetz thimbles.

However, the Morse–Smale condition for $\text{Re}(S)$ is not always satisfied in practical applications to physics. Especially for gauge theories, the set of critical points is usually degenerate due to the gauge symmetry. In this case, the above equivalence between the gradient flow and the Hamilton equation is very helpful by choosing the Kähler metric [40, 41] (see also [19, 20]). Let us call the symmetry group \mathcal{G} , then one can construct Noether charges Q for this symmetry. One can consider the reduced phase space by performing the symplectic reduction $Q^{-1}(0)/\mathcal{G}$ (also called Marsden–Weinstein reduction) [82], and define the Lefschetz-thimble decomposition in the reduced phase space. Using the Lefschetz thimbles and dual thimbles computed in $Q^{-1}(0)/\mathcal{G}$, one can construct correct half dimensional cycles in M by considering group actions of the Noether charge Q so that the intersection number is well-defined. From this argument, it turns out to be quite helpful to choose the Kähler metric instead of the Hermitian metric in order to prove the existence of the Lefschetz-thimble decomposition when the classical action S has continuous symmetries.

On the other hand, the two important properties, $\frac{d}{dt}\text{Re}(S) \geq 0$ and $\frac{d}{dt}\text{Im}(S) = 0$, are satisfied in general for Hermitian metrics. So long as one has a program to construct half-dimensional cycles using the flow, the Hermitian property is good enough to cure the sign

problem. Equation (2.11) provides such a method, and thus our choice of metric in (3.1) can be used also for theories with continuous symmetries, especially gauge theories.

References

- [1] F. Karsch, “Lattice QCD at high temperature and density,” *Lect.Notes Phys.* **583** (2002) 209–249, [arXiv:hep-lat/0106019 \[hep-lat\]](#).
- [2] D. M. Ceperley, “Path integrals in the theory of condensed helium,” *Rev. Mod. Phys.* **67** (1995) 279–355.
- [3] L. Pollet, “Recent developments in quantum Monte Carlo simulations with applications for cold gases,” *Rep. Prog. Phys.* **75** (2012) 094501, [arXiv:1206.0781 \[cond-mat.quant-gas\]](#).
- [4] A. Yamamoto and T. Hatsuda, “Quantum Monte Carlo simulation of three-dimensional Bose-Fermi mixtures,” *Phys. Rev. A* **86** (2012) 043627, [arXiv:1209.1954 \[cond-mat.quant-gas\]](#).
- [5] E. Y. Loh, J. E. Gubernatis, R. T. Scalettar, S. R. White, D. J. Scalapino, and R. L. Sugar, “Sign problem in the numerical simulation of many-electron systems,” *Phys. Rev. B* **41** (May, 1990) 9301–9307.
- [6] G. G. Batrouni and P. de Forcrand, “The Fermion sign problem: A New decoupling transformation, and a new simulation algorithm,” *Phys. Rev. B* **48** (1993) 589, [arXiv:cond-mat/9211009 \[cond-mat\]](#).
- [7] M. Troyer and U.-J. Wiese, “Computational complexity and fundamental limitations to fermionic quantum Monte Carlo simulations,” *Phys. Rev. Lett.* **94** (2005) 170201, [arXiv:cond-mat/0408370 \[cond-mat\]](#).
- [8] K. Fukushima and T. Hatsuda, “The phase diagram of dense QCD,” *Rep. Prog. Phys.* **74** (2011) 014001, [arXiv:1005.4814 \[hep-ph\]](#).
- [9] S. Muroya, A. Nakamura, C. Nonaka, and T. Takahashi, “Lattice QCD at finite density: An Introductory review,” *Prog. Theor. Phys.* **110** (2003) 615–668, [arXiv:hep-lat/0306031 \[hep-lat\]](#).
- [10] **AuroraScience** Collaboration, M. Cristoforetti, F. Di Renzo, and L. Scorzato, “New approach to the sign problem in quantum field theories: High density QCD on a Lefschetz thimble,” *Phys. Rev. D* **86** (2012) 074506, [arXiv:1205.3996 \[hep-lat\]](#).
- [11] M. Cristoforetti, F. Di Renzo, A. Mukherjee, and L. Scorzato, “Monte Carlo simulations on the Lefschetz thimble: taming the sign problem,” *Phys. Rev. D* **88** (2013) 051501, [arXiv:1303.7204 \[hep-lat\]](#).
- [12] M. Cristoforetti, F. Di Renzo, G. Erucci, A. Mukherjee, C. Schmidt, L. Scorzato, and C. Torrero, “An efficient method to compute the residual phase on a Lefschetz thimble,” *Phys. Rev. D* **89** (2014) 114505, [arXiv:1403.5637 \[hep-lat\]](#).
- [13] G. Aarts, “Lefschetz thimbles and stochastic quantisation: Complex actions in the complex plane,” *Phys. Rev. D* **88** (2013) 094501, [arXiv:1308.4811 \[hep-lat\]](#).
- [14] H. Fujii, D. Honda, M. Kato, Y. Kikukawa, S. Komatsu, and T. Sano, “Hybrid Monte Carlo on Lefschetz thimbles - A study of the residual sign problem,” *JHEP* **1310** (2013) 147, [arXiv:1309.4371 \[hep-lat\]](#).

- [15] A. Mukherjee and M. Cristoforetti, “Lefschetz thimble Monte Carlo for many body theories: application to the repulsive Hubbard model away from half filling,” *Phys. Rev. B* **90** (2014) 035134, [arXiv:1403.5680 \[cond-mat.str-el\]](#).
- [16] G. Aarts, L. Bongiovanni, E. Seiler, and D. Sexty, “Some remarks on Lefschetz thimbles and complex Langevin dynamics,” *JHEP* **1410** (2014) 159, [arXiv:1407.2090 \[hep-lat\]](#).
- [17] Y. Tanizaki and T. Koike, “Real-time Feynman path integral with Picard–Lefschetz theory and its applications to quantum tunneling,” *Ann. Phys.* **351** (2014) 250, [arXiv:1406.2386 \[math-ph\]](#).
- [18] A. Cherman and M. Unsal, “Real-Time Feynman Path Integral Realization of Instantons,” [arXiv:1408.0012 \[hep-th\]](#).
- [19] Y. Tanizaki, “Lefschetz-thimble techniques for path integral of zero-dimensional $O(n)$ sigma models,” *Phys. Rev. D* **91** (2015) 036002, [arXiv:1412.1891 \[hep-th\]](#).
- [20] T. Kanazawa and Y. Tanizaki, “Structure of Lefschetz thimbles in simple fermionic systems,” *JHEP* **1503** (2015) 044, [arXiv:1412.2802 \[hep-th\]](#).
- [21] Y. Tanizaki, H. Nishimura, and K. Kashiwa, “Evading the sign problem in the mean-field approximation through Lefschetz-thimble path integral,” *Phys. Rev. D* **91** (2015) 101701, [arXiv:1504.02979 \[hep-th\]](#).
- [22] F. Di Renzo and G. Erucci, “Thimble regularization at work: from toy models to chiral random matrix theories,” *Phys. Rev. D* **92** (2015) 085030, [arXiv:1507.03858 \[hep-lat\]](#).
- [23] K. Fukushima and Y. Tanizaki, “Hamilton dynamics for the Lefschetz thimble integration akin to the complex Langevin method,” *Prog. Theor. Exp. Phys.* **2015** (2015) 111A01, [arXiv:1507.07351 \[hep-th\]](#).
- [24] S. Tsutsui and T. M. Doi, “An improvement in complex Langevin dynamics from a view point of Lefschetz thimbles,” *Phys. Rev.* **D94** (2016) 074009, [arXiv:1508.04231 \[hep-lat\]](#).
- [25] Y. Tanizaki, Y. Hidaka, and T. Hayata, “Lefschetz-thimble analysis of the sign problem in one-site fermion model,” *New J. Phys.* **18** (2016) 033002, [arXiv:1509.07146 \[hep-th\]](#).
- [26] H. Fujii, S. Kamata, and Y. Kikukawa, “Lefschetz thimble structure in one-dimensional lattice Thirring model at finite density,” *JHEP* **11** (2015) 078, [arXiv:1509.08176 \[hep-lat\]](#). [Erratum: JHEP02,036(2016)].
- [27] H. Fujii, S. Kamata, and Y. Kikukawa, “Monte Carlo study of Lefschetz thimble structure in one-dimensional Thirring model at finite density,” *JHEP* **12** (2015) 125, [arXiv:1509.09141 \[hep-lat\]](#).
- [28] A. Alexandru, G. Basar, and P. Bedaque, “Monte Carlo algorithm for simulating fermions on Lefschetz thimbles,” *Phys. Rev.* **D93** (2016) 014504, [arXiv:1510.03258 \[hep-lat\]](#).
- [29] T. Hayata, Y. Hidaka, and Y. Tanizaki, “Complex saddle points and the sign problem in complex Langevin simulation,” *Nucl. Phys.* **B911** (2016) 94–105, [arXiv:1511.02437 \[hep-lat\]](#).
- [30] A. Alexandru, G. Basar, P. F. Bedaque, G. W. Ridgway, and N. C. Warrington, “Sign problem and Monte Carlo calculations beyond Lefschetz thimbles,” *JHEP* **05** (2016) 053, [arXiv:1512.08764 \[hep-lat\]](#).
- [31] A. Alexandru, G. Basar, P. F. Bedaque, S. Vartak, and N. C. Warrington, “Monte Carlo

- Study of Real Time Dynamics on the Lattice,” *Phys. Rev. Lett.* **117** (2016) 081602, [arXiv:1605.08040 \[hep-lat\]](#).
- [32] A. Alexandru, G. Basar, P. F. Bedaque, G. W. Ridgway, and N. C. Warrington, “Monte Carlo calculations of the finite density Thirring model,” *Phys. Rev.* **D95** (2017) 014502, [arXiv:1609.01730 \[hep-lat\]](#).
- [33] Y. Tanizaki and M. Tachibana, “Multi-flavor massless QED₂ at finite densities via Lefschetz thimbles,” *JHEP* **02** (2017) 081, [arXiv:1612.06529 \[hep-th\]](#).
- [34] M. Fukuma and N. Umeda, “Parallel tempering algorithm for the integration over Lefschetz thimbles,” [arXiv:1703.00861 \[hep-lat\]](#).
- [35] A. Alexandru, G. Basar, P. F. Bedaque, and N. C. Warrington, “Tempered transitions between thimbles,” [arXiv:1703.02414 \[hep-lat\]](#).
- [36] J. Nishimura and S. Shimasaki, “Combining the complex Langevin method and the generalized Lefschetz-thimble method,” [arXiv:1703.09409 \[hep-lat\]](#).
- [37] F. Pham, “Vanishing homologies and the n variable saddlepoint method,” in *Proc. Symp. Pure Math*, vol. 40.2, pp. 319–333. AMS, 1983.
- [38] D. Kaminski, “Exponentially improved stationary phase approximations for double integrals,” *Methods and Appl. of Analysis* **1** (1994) 44–56.
- [39] C. J. Howls, “Hyperasymptotics for multidimensional integrals, exact remainder terms and the global connection problem,” *Proc. R. Soc. A* **453** no. 1966, (1997) 2271–2294.
- [40] E. Witten, “Analytic Continuation Of Chern-Simons Theory,” in *Chern-Simons Gauge Theory: 20 Years After*, vol. 50, pp. 347–446. AMS/IP Stud. Adv. Math., 2010. [arXiv:1001.2933 \[hep-th\]](#).
- [41] E. Witten, “A New Look At The Path Integral Of Quantum Mechanics,” [arXiv:1009.6032 \[hep-th\]](#).
- [42] D. Harlow, J. Maltz, and E. Witten, “Analytic Continuation of Liouville Theory,” *JHEP* **1112** (2011) 071, [arXiv:1108.4417 \[hep-th\]](#).
- [43] G. V. Dunne and M. Unsal, “Resurgence and Trans-series in Quantum Field Theory: The CP(N-1) Model,” *JHEP* **11** (2012) 170, [arXiv:1210.2423 \[hep-th\]](#).
- [44] G. Basar, G. V. Dunne, and M. Ünsal, “Resurgence theory, ghost-instantons, and analytic continuation of path integrals,” *JHEP* **1310** (2013) 041, [arXiv:1308.1108 \[hep-th\]](#).
- [45] A. Cherman, D. Dorigoni, and M. Unsal, “Decoding perturbation theory using resurgence: Stokes phenomena, new saddle points and Lefschetz thimbles,” *JHEP* **10** (2015) 056, [arXiv:1403.1277 \[hep-th\]](#).
- [46] A. Cherman, P. Koroteev, and M. Ünsal, “Resurgence and Holomorphy: From Weak to Strong Coupling,” *J. Math. Phys.* **56** no. 5, (2015) 053505, [arXiv:1410.0388 \[hep-th\]](#).
- [47] D. Dorigoni, “An Introduction to Resurgence, Trans-Series and Alien Calculus,” [arXiv:1411.3585 \[hep-th\]](#).
- [48] G. Felder and R. Riser, “Holomorphic matrix integrals,” *Nucl.Phys.* **B691** (2004) 251–258, [arXiv:hep-th/0401191 \[hep-th\]](#).
- [49] M. Marino, “Nonperturbative effects and nonperturbative definitions in matrix models and topological strings,” *JHEP* **12** (2008) 114, [arXiv:0805.3033 \[hep-th\]](#).

- [50] M. Mariño, “Lectures on non-perturbative effects in large N gauge theories, matrix models and strings,” *Fortsch. Phys.* **62** (2014) 455–540, [arXiv:1206.6272 \[hep-th\]](#).
- [51] R. Schiappa and R. Vaz, “The Resurgence of Instantons: Multi-Cut Stokes Phases and the Painleve II Equation,” *Commun. Math. Phys.* **330** (2014) 655–721, [arXiv:1302.5138 \[hep-th\]](#).
- [52] T. Misumi, M. Nitta, and N. Sakai, “Classifying bions in Grassmann sigma models and non-Abelian gauge theories by D-branes,” *PTEP* **2015** (2015) 033B02, [arXiv:1409.3444 \[hep-th\]](#).
- [53] T. Misumi, M. Nitta, and N. Sakai, “Neutral bions in the $\mathbb{C}P^{N-1}$ model,” *JHEP* **06** (2014) 164, [arXiv:1404.7225 \[hep-th\]](#).
- [54] A. Behtash, T. Sulejmanpasic, T. Schäfer, and M. Ünsal, “Hidden Topological Angles in Path Integrals,” *Phys. Rev. Lett.* **115** no. 4, (2015) 041601, [arXiv:1502.06624 \[hep-th\]](#).
- [55] A. Behtash, E. Poppitz, T. Sulejmanpasic, and M. Ünsal, “The curious incident of multi-instantons and the necessity of Lefschetz thimbles,” *JHEP* **11** (2015) 175, [arXiv:1507.04063 \[hep-th\]](#).
- [56] G. Basar and G. V. Dunne, “Resurgence and the Nekrasov-Shatashvili limit: connecting weak and strong coupling in the Mathieu and Lamé systems,” *JHEP* **02** (2015) 160, [arXiv:1501.05671 \[hep-th\]](#).
- [57] A. Cherman, T. Schafer, and M. Unsal, “Chiral Lagrangian from Duality and Monopole Operators in Compactified QCD,” *Phys. Rev. Lett.* **117** no. 8, (2016) 081601, [arXiv:1604.06108 \[hep-th\]](#).
- [58] S. Gukov, M. Marino, and P. Putrov, “Resurgence in complex Chern-Simons theory,” [arXiv:1605.07615 \[hep-th\]](#).
- [59] S. Gukov, “RG Flows and Bifurcations,” [arXiv:1608.06638 \[hep-th\]](#).
- [60] T. Fujimori, S. Kamata, T. Misumi, M. Nitta, and N. Sakai, “Nonperturbative contributions from complexified solutions in $\mathbb{C}P^{N-1}$ models,” *Phys. Rev.* **D94** no. 10, (2016) 105002, [arXiv:1607.04205 \[hep-th\]](#).
- [61] C. Kozcaz, T. Sulejmanpasic, Y. Tanizaki, and M. Unsal, “Cheshire Cat resurgence, Self-resurgence and Quasi-Exact Solvable Systems,” [arXiv:1609.06198 \[hep-th\]](#).
- [62] T. Sulejmanpasic, “Global Symmetries, Volume Independence, and Continuity in Quantum Field Theories,” *Phys. Rev. Lett.* **118** no. 1, (2017) 011601, [arXiv:1610.04009 \[hep-th\]](#).
- [63] J. Feldbrugge, J.-L. Lehners, and N. Turok, “No smooth beginning for spacetime,” [arXiv:1705.00192 \[hep-th\]](#).
- [64] J. Diaz Dorronsoro, J. J. Halliwell, J. B. Hartle, T. Hertog, and O. Janssen, “The Real No-Boundary Wave Function in Lorentzian Quantum Cosmology,” [arXiv:1705.05340 \[gr-qc\]](#).
- [65] J. Nishimura and S. Shimasaki, “New insights into the problem with a singular drift term in the complex Langevin method,” *Phys. Rev. D* **92** (2015) 011501, [arXiv:1504.08359 \[hep-lat\]](#).
- [66] G. Aarts, E. Seiler, and I.-O. Stamatescu, “The Complex Langevin method: When can it be trusted?,” *Phys. Rev. D* **81** (2010) 054508, [arXiv:0912.3360 \[hep-lat\]](#).

- [67] G. Aarts, F. A. James, E. Seiler, and I.-O. Stamatescu, “Complex Langevin: Etiology and Diagnostics of its Main Problem,” *Eur. Phys. J. C* **71** (2011) 1756, [arXiv:1101.3270 \[hep-lat\]](#).
- [68] K. Nagata, J. Nishimura, and S. Shimasaki, “Argument for justification of the complex Langevin method and the condition for correct convergence,” *Phys. Rev.* **D94** no. 11, (2016) 114515, [arXiv:1606.07627 \[hep-lat\]](#).
- [69] Y. Abe and K. Fukushima, “Analytic studies of the complex Langevin equation with a Gaussian ansatz and multiple solutions in the unstable region,” *Phys. Rev.* **D94** no. 9, (2016) 094506, [arXiv:1607.05436 \[hep-lat\]](#).
- [70] L. L. Salcedo, “Does the complex Langevin method give unbiased results?,” *Phys. Rev.* **D94** no. 11, (2016) 114505, [arXiv:1611.06390 \[hep-lat\]](#).
- [71] P. E. Gibbs, “Lattice Monte Carlo Simulations of QCD at Finite Baryonic Density,” *Phys. Lett.* **B182** (1986) 369–372.
- [72] P. E. Gibbs, “The Fermion Propagator Matrix in Lattice QCD,” *Phys. Lett.* **B172** (1986) 53–61.
- [73] I. M. Barbour, S. E. Morrison, E. G. Klepfish, J. B. Kogut, and M.-P. Lombardo, “The Critical points of strongly coupled lattice QCD at nonzero chemical potential,” *Phys. Rev.* **D56** (1997) 7063–7072, [arXiv:hep-lat/9705038 \[hep-lat\]](#).
- [74] I. M. Barbour, S. E. Morrison, E. G. Klepfish, J. B. Kogut, and M.-P. Lombardo, “Results on finite density QCD,” *Nucl. Phys. Proc. Suppl.* **60A** (1998) 220–234, [arXiv:hep-lat/9705042 \[hep-lat\]](#).
- [75] M. A. Stephanov, “Random matrix model of QCD at finite density and the nature of the quenched limit,” *Phys. Rev. Lett.* **76** (1996) 4472–4475, [arXiv:hep-lat/9604003 \[hep-lat\]](#).
- [76] T. D. Cohen, “Functional integrals for QCD at nonzero chemical potential and zero density,” *Phys. Rev. Lett.* **91** (2003) 222001, [arXiv:hep-ph/0307089 \[hep-ph\]](#).
- [77] K. Splittorff and J. J. M. Verbaarschot, “Phase of the Fermion Determinant at Nonzero Chemical Potential,” *Phys. Rev. Lett.* **98** (2007) 031601, [arXiv:hep-lat/0609076 \[hep-lat\]](#).
- [78] K. Splittorff and J. J. M. Verbaarschot, “The QCD Sign Problem for Small Chemical Potential,” *Phys. Rev.* **D75** (2007) 116003, [arXiv:hep-lat/0702011 \[HEP-LAT\]](#).
- [79] A. Cherman, M. Hanada, and D. Robles-Llana, “Orbifold equivalence and the sign problem at finite baryon density,” *Phys. Rev. Lett.* **106** (2011) 091603, [arXiv:1009.1623 \[hep-th\]](#).
- [80] Y. Hidaka and N. Yamamoto, “No-Go Theorem for Critical Phenomena in Large-Nc QCD,” *Phys. Rev. Lett.* **108** (2012) 121601, [arXiv:1110.3044 \[hep-ph\]](#).
- [81] **XQCD-J** Collaboration, K. Nagata, S. Motoki, Y. Nakagawa, A. Nakamura, and T. Saito, “Towards extremely dense matter on the lattice,” *Prog. Theor. Exp. Phys.* **2012** (2012) 01A103, [arXiv:1204.1412 \[hep-lat\]](#).
- [82] V. Arnold, *Mathematical Methods of Classical Mechanics*. Graduate Texts in Mathematics Vol.60. Springer, 2nd ed., 1989. translated by K. Vogtmann and A.Weinstein.